HHS Public Access

Author manuscript

Nano Res. Author manuscript; available in PMC 2019 October 01.

Published in final edited form as:

Nano Res. 2018 October ; 11(10): 4955–4984. doi:10.1007/s12274-018-2092-y.

Scavenging of reactive oxygen and nitrogen species with nanomaterials

Carolina A. Ferreira, **Dalong Ni**✉, **Zachary T. Rosenkrans**, and **Weibo Cai**✉

Department of Radiology, University of Wisconsin-Madison, Madison, WI 53705, USA

Abstract

Reactive oxygen and nitrogen species (RONS) are essential for normal physiological processes and play important roles in cell signaling, immunity, and tissue homeostasis. However, excess radical species are implicated in the development and augmented pathogenesis of various diseases. Several antioxidants may restore the chemical balance, but their use is limited by disappointing results of clinical trials. Nanoparticles are an attractive therapeutic alternative because they can change the biodistribution profile of antioxidants, and possess intrinsic ability to scavenge RONS. Herein, we review the types of RONS, how they are implicated in several diseases, and the types of nanoparticles with inherent antioxidant capability, their mechanisms of action, and their biological applications.

Keywords

mnanomaterials; reactive oxygen species (ROS); reactive nitrogen species; ROS scavenging; antioxidant nanoparticles

1 Introduction

Reactive oxygen species (ROS) were discovered in biological environments in 1954 [1]. Since then, ROS have been the target of intense research, examining their chemical and physiological activity, and their pathological roles in living organisms [2]. ROS is a general term used to describe free radicals, a species containing one or more unpaired electrons of oxygen, such as hydroxyl ($^{\bullet}OH$) and superoxide ($O_2^{\bullet-}$), as well as nonradical oxidizing agents that are easily converted into radicals such as hydrogen peroxide (H_2O_2) and hypochlorous acid (HOCl) [3]. The term reactive oxygen and nitrogen species (RONS) is employed to further encompass this class of chemically reactive molecules that contain nitrogen or reactive nitrogen species (RNS) such as nitric oxide ($NO^{\bullet}$) and peroxynitrite ($ONOO^-$). In general, RONS have a very short life, in the order of micro- or nanoseconds, and readily react with numerous cellular components including lipids, nucleic acids, and proteins. This process, which occurs via a free-radical chain reaction, causes damage and forms harmful secondary products such as lipid peroxides and other lipid adducts. The subsequent protein damage results in loss of enzyme activity, while DNA damage results in mutagenesis and carcinogenesis [4].

Address correspondence to Dalong Ni, dni2@wisc.edu; Weibo Cai, wcai@uwhealth.org.

Redox regulators and mediators may be interconnected with the normal function of the cell and its surroundings, comprising a type of complex network that can affect the energetic state, metabolism, state of health, disease, and even lifespan of the entire organism [2]. Thus, RONS homeostasis is imperative for normal cell survival and proper cell signaling. Cells regulate intracellular ROS levels in a spatial and temporal manner via an extensive antioxidant defense system. For example, O_2^- is degraded by the enzyme superoxide dismutase (SOD), present in various cellular compartments, in a dismutation reaction yielding H_2O_2 and O_2 [5]. To prevent cellular toxicity and maintain H_2O_2 levels in the range optimal for cell signaling, numerous antioxidants, such as peroxiredoxins (PRXs), glutathione peroxidases (GPXs), and catalase (CAT), convert intracellular H_2O_2 into water (H_2O) [6]. Physiologically, these mechanisms cannot entirely eradicate all the RONS produced. This innate physiological process, in which the presence of RONS overpowers the radical-scavenging mechanisms, is called “oxidative stress”. Oxidative stress creates an imbalance between the oxidants and the antioxidants, and is implicated in aging [7].

Disturbances in RONS signaling leads to their overproduction or lower levels of detoxification, resulting in an altered redox state that can cause oxidative damage to cell components. The presence of RONS is implicated in various diseases such as stroke [8], sepsis [9], diabetes [10], hypertension [11], neurodegenerative diseases [12], inflammation [13], and cancer [14]. Restoration of proper RONS concentration, by either regulating their intracellular production or targeting their inactivation, may provide a new therapeutic paradigm for treating ROS-linked diseases. Several antioxidants have been investigated for their therapeutic potential. These include nitroxide radical compounds (ex. Tempo, Tempol, Tempamine) [15]; superoxide dismutase mimics [16]; endogenous natural antioxidants, such as vitamins (ex. α-tocopherol) and flavonoids [17]; primary and secondary enzymes such as SOD, catalases, and glutathione peroxidases; and nonenzymatic antioxidants such as carotenoids, cofactors, and polyphenols [18]. However, the results of clinical trials with antioxidants have shown that antioxidants fail to prevent the progression of ROS-associated diseases, have few benefits [19–24], and exert severe side effects at high doses [25]. These disappointing results may have several possible explanations: high renal clearance, low bioavailability, non-optimal time and duration of therapy, metabolite toxicity, physiological mechanisms that prevent high tissue concentrations, and toxicity [17]. Perhaps most importantly, these antioxidants show poor target specificity and nonspecific dispersion in normal tissues [26].

Nanoparticles (NPs), which have emerged as an alternative strategy for scavenging RONS *in vivo*, may overcome these limitations. This is because NPs can engineer, control, and influence the biodistribution and specificity of known antioxidants, while in some cases harboring inherent antioxidant properties. Different types of nanoparticles, mostly inorganic, often possess intrinsic catalytic properties, which are enhanced by their relatively large surface areas [27]; such nanoparticles can directly react with RONS, mimicking the natural RONS-scavenging capability of cellular enzymes. Here, we provide a comprehensive review on: (i) the types of RONS found in living organisms; (ii) mechanisms by which RONS cause damage to biological molecules; (iii) types of nanoparticles, such as ceria, carbon, manganese, and platinum nanoparticles, that have been used as RONS-scavenging agents;

(iv) and RONS-associated diseases including sepsis, stroke, neurodegenerative and inflammatory diseases, diabetes, and cancer.

2 Classification of reactive oxygen nitrogen species

Reactive species, or free radicals, are a group of highly reactive chemical molecules with one or more unpaired electrons. These molecules arise from chain reactions that include three steps: initiation, propagation, and termination. In this manner, formation of free radicals is able to trigger amplification. Collectively, reactive species, present in living organisms, are called RONS and are separated into three groups: oxygen-centered (ROS), nitrogen-centered (RNS), and others including non-radicals that are either oxidizing agents or easily converted into radicals (Fig. 1) [4]. RONS are formed as natural byproducts of normal cellular metabolism and are released by specific cell types (macrophages, neutrophils, and dendritic cells) in response to external stimuli, such as inflammation [28]. The next section briefly describes the types of reactive species, the mechanisms by which they are produced *in vivo*, and their physiological and pathological roles.

2.1 Reactive oxygen species

2.1.1 $O_2^{\bullet -}$—The $O_2^{\bullet -}$ is the most common RONS, mainly generated via conversion of a small percentage of oxygen molecules (1%–2%) that are not reduced to water in the mitochondrial electron transport chain (ETC) [3, 10]. Mitochondria are the main intracellular source of $O_2^{\bullet -}$, which is formed by a single-electron reduction of oxygen (equation shown below), a side reaction of the respiratory chain [11]. This process is mediated by enzymes such as dihydronicotinamide-adenine dinucleotide phosphate (NAD(P)H), oxidases, and xanthine oxidase, or non-enzymatically by redox-reactive compounds such as the semi-ubiquinone compound of the ETC [29].

$$O_2 + 1e^- + H^+ \leftrightarrow HO_2^{\bullet} \leftrightarrow H^+ + O_2^{\bullet -}$$

Another important pathway for forming the superoxide is via heme oxidation (equation shown below). The iron of the heme group in deoxyhemoglobin is reduced to ferrous (Fe^{2+}) and forms an intermediate when complexed with oxygen [28], as shown

$$\text{Heme } Fe^{2+} - O_2^- \leftrightarrow O_2^{\bullet -} + \text{Heme } Fe^{3+}$$

$O_2^{\bullet -}$ can also generate secondary ROS by interacting with other molecules and acting as both an oxidizing and reducing agent [28]

$$\left.\begin{array}{l} O_2 + 1e^- + H^+ \leftrightarrow HO_2^{\bullet} \leftrightarrow H^+ + O_2^{\bullet -} \\ HO_2^{\bullet} + 1e^- + H^+ \leftrightarrow H_2O_2 \end{array}\right| X + O_2^{\bullet -} + H^+ \rightarrow XH + O_2$$

$$\left.\begin{array}{l} H_2O_2 + 1e^- + H^+ \leftrightarrow [H_3O_2] \leftrightarrow H_2O + {}^{\bullet}OH \\ {}^{\bullet}OH + 1e^- + H^+ \leftrightarrow H_2O \end{array}\right| YH + O_2^{\bullet -} + H^+ \rightarrow Y^{\bullet} + H_2O_2$$

The removal of excess RONS is an important defense mechanism in aerobic organisms [30]. Every cell has antioxidant mechanisms that can be classified as enzymatic or nonenzymatic depending on their action in intracellular and extracellular compartments. Nonenzymatic antioxidant defenses act indiscriminately on RONS and include mostly molecules with low molecular weight. Examples of such compounds are glutathione, uric acid, vitamin A (retinoids), and carotenoids such as beta carotene and α-tocopherol (vitamin E); α-tocopherol is a fat-soluble and free radical chain-breaking antioxidant that is an effective hydrogen donor due to the presence of a hydroxyl (–OH) group. Fukuzawa has shown that, under physiological conditions, α-tocopherol micelles at various concentrations can inactivate up to 99% of $O_2^{\bullet -}$ [31]. Other molecules that can also reduce or inhibit the generation of RONS include bilirubin, lipoic acid, albumin, ferritin, ceruloplasmin, and transferrin [4]. Enzymatic antioxidants act more specifically on each RONS. In the case of $O_2^{\bullet}$, the enzyme SOD plays a major role in regulating the intracellular concentration of $O_2^{\bullet}$. SOD, found as isoforms (copper/zinc SOD, mitochondrial SOD, and extracellular SOD) in mammals, catalyzes the dismutation of $O_2^{\bullet -}$ into H_2O and O_2 [32].

2.1.2 H_2O_2—H_2O_2, a two-electron oxidant, reacts poorly or not at all with most biological molecules, including low-molecular-weight antioxidants. H_2O_2, which reacts slowly with thiols, reacts mainly with seleno-, thiol, or heme peroxidases, or other transition metal centers, yielding both radical and nonradical species. H_2O_2 is an oxidizing agent with poor reactivity, but unlike the superoxide anion, H_2O_2 can easily cross cell membranes [3]. The biologically damaging effects are mainly due to secondary products and hydroxyl radicals formed by Fenton chemistry [33].

The dismutation reaction of hydrogen peroxide is catalyzed by catalase, an enzyme that is present in the liver, kidney, blood, and almost all animal tissues. However, hydrogen peroxide is most efficiently scavenged by the enzyme GPx, which requires glutathione (GSH) as the electron donor. The oxidized glutathione is then converted back to GSH by the enzyme glutathione reductase (with NADPH as the electron donor). Certain transition metals, such as Fe^{2+} and Cu^{+}, can also break down hydrogen peroxide, generating the reactive hydroxyl radical. Lastly, peroxiredoxins, a recently identified group of enzymes, reduce the levels of hydrogen peroxide, lipid peroxides, and organic hydroperoxides. Each of these protein catalysts, generally found in one subcellular compartment, plays a specific role in maintaining the proper peroxide levels required for protecting the cell against oxidative damage, while allowing peroxides to serve as key signaling molecules in regulation of gene expression and enzymatic activities [34].

2.1.3 $^{\bullet}OH$—The $^{\bullet}OH$ is the most reactive radical among all RONS. Because of this, the hydroxyl radical usually reacts close to its site of formation and has a very short *in vivo* half-life of approximately 10^{-9} s [35]. The hydroxyl radicals react strongly with both organic and inorganic molecules, including DNA, proteins, lipids, and carbohydrates, and cause more damage to the cell than any other ROS [36]. Hydroxyl radicals are primarily produced via the Haber–Weiss reaction of excess superoxide anions or hydrogen peroxide [37]

$$O_2^{\bullet -} + H_2O \rightarrow OH^{-} + {}^{\bullet}OH + O_2$$

In vivo, radical species can also be formed from the metal-catalyzed breakdown of hydrogen peroxide via the Fenton reaction [38]

$$M^{n+} + H_2O_2 \rightarrow M^{(n+1)} + OH^- + {}^{\bullet}OH$$

where M^{n+} is a transitional metal ion such as Cu^+, Fe^{2+}, Ti^{3+}, or Co^{2+}. Hydroxyl radicals can also be generated by various mechanisms such as ionizing radiation, which causes decomposition of water and results in the formation of OH and hydrogen atoms, or by photolytic decomposition of alkylhydroperoxides [38]. Reactions of $^{\bullet}OH$ can be classified into three categories: hydrogen abstraction, addition, and electron transfer reactions. $^{\bullet}OH$ rapidly abstracts hydrogen atoms from organic compounds, especially from those that are weakly bound. The reaction produces H_2O and a carbon-centered radical ($RC^{\bullet}$), which generates peroxyl radicals ($ROO^{\bullet}$) in the presence of O_2, such as carbon-centered lipid radicals. In the absence of O_2, a covalent bond can be formed between two $RC^{\bullet}$, producing a crosslink. An example is the reaction between two $Tyr^{\bullet}$ to produce dityrosine. Reactions of $^{\bullet}OH$ with aromatic compounds usually involve the addition of the radical to produce hydroxylated radical adducts. An important example is the addition of $^{\bullet}OH$ to the guanine moiety of DNA/RNA to produce 8-hydroxyguanine and 2,6-diamino-4-hydroxy-5-formamidopyrimidine [39].

2.2 Reactive nitrogen species

2.2.1 $NO^{\bullet}$—$NO^{\bullet}$ is involved in cellular signaling, vasodilation, and the immune response. Nitric oxide has a half-life of 15 s and, because it is uncharged, can easily diffuse across cellular membranes. Endogenous $NO^{\bullet}$ is generated through the conversion of L-arginine and oxygen into $NO^{\bullet}$ and citrulline, catalyzed by the enzyme nitric oxide synthase (NOS). This reaction requires the presence of cofactors such as flavin adenine dinucleotide (FAD), flavin mononucleotide (FMN), NADPH, tetrahydrobiopterin, and heme. Under uncoupling conditions, these enzymes also produce superoxide [4]

$$\text{NOS} + \text{L} - \text{arginine} + O_2{}^{\bullet -} + \text{NADPH} \rightarrow NO^{\bullet} + \text{citrulline} + NADP^+$$

$$\text{NOS (Fe(II) heme)} + O_2{}^{\bullet -} \rightarrow \text{NOS (Fe(III) heme)} + O_2{}^{\bullet -}$$

Unlike other signaling molecules that act through receptors, the produced $NO^{\bullet}$ diffuses out of the cell and to target cells; $NO^{\bullet}$ then transmits signals that interact with molecular targets including proteins, nucleic acids, and other free radicals such as superoxide [40]. The direct action of $NO^{\bullet}$ is limited by its biologic half-life *in vivo* (1 s) and the resulting short distance that this molecule can traverse. Under conditions of physiological stress, $NO^{\bullet}$ binds to the heme iron of guanylyl cyclase (GC) and activates the GC- and cyclic guanosine 3',5'-monophosphate (cGMP)-dependent pathways. The $NO^{\bullet}$ released from endothelial cells diffuses toward the neighboring smooth muscle cells and activates GC. The produced cGMP interacts with protein kinase G (PKG), which phosphorylates contractile proteins, decreases

the levels of cytosolic Ca^{2+}, generates dephosphorylation of the myosin light chain, and induces vasorelaxation [41].

2.2.2 $OONO^-$—More reactive than $NO^\bullet$, $OONO^-$ is an RNS generated from the rapid reaction between $NO^\bullet$ and $O_2^{\bullet-}$. Peroxynitrite is a strong oxidant that mainly nitrates tyrosine residues in nonenzymatic reactions. In biologic systems, $OONO^-$ rapidly reacts with CO_2 (in equilibrium with physiologic levels of HCO_3^-), which leads to the formation of $CO_3^{\bullet-}$ and $NO_2^{\bullet-}$ radicals that oxidate and nitrate proteins [41]. $OONO^-$ can produce other radicals by mediating one-electron transfer reactions. In lipids, this results in initiation of self-sustaining peroxidation reactions. Peroxynitrite is also reactive with all the major classes of biomolecules, and thereby can potentially mediate cytotoxicity independently of NO or $O_2^{\bullet-}$ [42].

2.3 Others

2.3.1 Hydroperoxyl ($HO_2^\bullet$)—$HO_2^\bullet$ or the hydroperoxyl radical is the protonated form of $O_2^{\bullet-}$; both species exist in equilibrium (pKa ~ 4.8). In the cytosol, approximately 0.3% of any superoxide is present in the protonated form [43]. Because $HO_2^\bullet$ is present in all compartments where superoxide anions are present, this radical must be considered when the subject is a biological environment.

2.3.2 Hypochlorous acid (HOCl)—HOCl and related species (HOX, X= Cl, Br, I, and SCN) are two moderately strong two electron oxidants. HOCl is a powerful oxidizing agent that can react with many biological molecules. HOCl and related species are primarily produced from the reactions of H_2O_2 with halide and pseudo-halide ions (Cl−, Br−, I− and SCN−) These reactions are catalyzed by myeloperoxidase (MPO) and eosinophil peroxidase in phagocytic cells [39]. Thiol groups and thioesters, such as methionine, are the ones most readily oxidized at a rate approximately 100 times that of amine groups. HOCl can also halogenate cell constituents. The most favored chlorinating reaction of HOCl is with amines, forming monochloramines and dichloramines. For that reason, proteins are a major target for HOCl. Additionally, HOCl can react with nucleotides and DNA. HOCl reacts rapidly with dihydronicotinamide-adenine dinucleotide (NADH) and the NH-groups of pyrimidines, slowly denatures DNA, induces DNA double-strand breaks, and generates modified nucleotides in cell lines exposed to HOCl. Another possible consequence of chloramine formation is the generation of radicals that may result in protein fragmentation or lipid peroxidation [44].

2.3.3 Singlet oxygen ($^1O_2$)—Singlet oxygen can be generated by an input of energy that rearranges the electrons. In both forms of singlet oxygen, the spin restriction is removed, which increases its oxidizing capacity. $^1O_2$ can directly oxidize proteins, DNA, and lipids. It is generated by chemical processes such as spontaneous decomposition of hydrogen trioxide in water or the reaction of hydrogen peroxide with hypochlorite. Singlet oxygen reacts with an alkene by abstraction of the allylic proton; this occurs in via ene-type reaction with the allyl hydroperoxide HO–O–R, which can then be reduced to the allyl alcohol [38].

2.3.4 Peroxyl ($RO_2^{\bullet}$) and alkoxyl ($RO^{\bullet}$) radicals—Peroxyl and alkoxyl radicals are good oxidizing agents, having more than 1,000 mV of standard reduction potential; this allows them to abstract hydrogen from other molecules. This reaction is frequently observed in the propagation stage of lipid peroxidation, forming an alkyl radical that can readily react with oxygen to form another $RO_2^{\bullet}$ and resulting in a chain reaction. Some peroxyl radicals break down to liberate the superoxide anion or react with each other to generate singlet oxygen. $RO_2^{\bullet}$ are formed by a direct reaction of oxygen with alkyl radicals ($R^{\bullet}$); an example of this is the reaction between lipid radicals and oxygen. Decomposition of alkyl peroxides (ROOH) also results in $RO_2^{\bullet}$ and $RO^{\bullet}$ radicals. UV light or transition-metal ions can trigger the conversion (homolysis) of peroxides into peroxyl and alkoxyl radicals, according to the reaction: $ROOH \rightarrow ROO^{\bullet} + H^{\bullet}$, $ROOH + Fe^{3+} \rightarrow ROO^{\bullet} + Fe^{2+} + H^{+}$ [45].

The main routes of RONS generation are represented in Fig. 2.

3 Oxidative damage by RONS

Enhanced levels of RONS can be detrimental to a diverse range of biomolecules, especially lipids, proteins, and DNA. The possible outcomes are altered membrane properties affecting fluidity or ion transport, loss of enzyme activity, inhibition of protein synthesis, DNA damage, and ultimately cell death [47]. The role of RONS in damage to biological molecules is discussed in the following sections.

3.1 Damage to DNA

RONS can cause DNA damage via several pathways that include: degradation of bases; single- or double-stranded DNA breaks; purine, pyrimidine, or sugar-bound modifications; mutations, deletions or translocations; and crosslinking with proteins [48]. Because of its proximity to generated RONS, mitochondrial DNA is more vulnerable to attack by RONS than is nuclear DNA. The $OH^{\bullet}$ radical abstracts hydrogen atoms and produces modified purines, pyrimidine base byproducts, and DNA–protein crosslinks. The pyrimidine attack by $OH^{\bullet}$ produces various pyrimidine adducts such as thymine glycol, uracil glycol, 5-hydroxydeoxy uridine, 5-hydroxy deoxycytidine, and hydantoin. The purine adducts, generated by an attack of a hydroxyl radical, include 8-hydroxy deoxy adenosine, 2,6-diamino-4-hydroxy-5-formamidopyrimidine, and 8-hydroxydeoxy guanosine (8-OH-G), which is a biomarker for carcinogenesis. Other free radical-induced adducts of DNA bases include 5-formyl uracil, cytosine glycol, 5,6-dihydrothyronine, 5-hydroxy-6-hydro-cytosine, 5-hydroxy-6-hydro uracil, uracil glycol, and alloxan [49]. These transcription factor-binding sites of promoter regions in the DNA are also susceptible to oxidative stress. Formation of altered bases in these sites can modify the binding of transcription factors and thereby change the expression of related genes [48].

3.2 Damage to lipids

Membrane lipids, especially the polyunsaturated fatty acid residues of phospholipids, are perhaps the most susceptible to oxidation by free radicals. RONS can induce lipid peroxidation and disrupt the arrangement of membrane lipid bilayer. This may inactivate membrane-bound receptors and enzymes, and increase tissue permeability. Lipid

peroxidation is initiated when free radicals attack and abstract hydrogen from the methylene groups (CH_2) in a fatty acid (LH). This results in formation of a carbon-centered lipid radical ($L^{\bullet}$) that can react with O_2, generating a lipid peroxyl radical ($LOO^{\bullet}$). The $LOO^{\bullet}$ undergoes rearrangement via a cyclization reaction to form endoperoxides, which finally form malondialdehyde (MDA) and 4-hydroxylnonenal (4-HNA). These toxic end products of lipid peroxidation are responsible for the damage to DNA and proteins [50].

3.3 Damage to proteins

Protein oxidation can be induced by radical species, such as $O_2^{\bullet-}$, $OH^{\bullet}$, $RO_2^{\bullet}$, $RO^{\bullet}$, and $HO_2^{\bullet}$, as well as by nonradical species such as H_2O_2, O_3, HOCl, $^1O_2$, and $OONO^-$. RONS can cause breakage of peptide chains, changes in protein electrical charge, protein–protein crosslinks, and oxidation of certain amino acids, leading to increased susceptibility to proteolysis via specific proteases [51]. RONS oxidize the different amino acids present in proteins. This causes the formation of protein–protein cross linkages and can ultimately result in loss of protein activity [52]. Additionally, there are certain groups that are more susceptible to oxidation from RONS. These include the amino acids cysteine and methionine or enzymes that have metals on or close to their active sites. The RONS-induced oxidative damage to amino acid residues, such as lysine, proline, threonine, and arginine, yields carbonyl derivatives. Therefore, the presence of carbonyl groups in proteins is considered a marker of RONS-mediated protein oxidation [53].

4 Nanomaterials to scavenge RONS

Oxidative stress, increased production of RONS, and insufficient protection by endogenous antioxidants are implicated in many types of diseases. Exogenous RONS scavengers, which are mostly synthetic and/or natural low-molecular-weight compounds, may be potential therapeutic agents [17]. However, problems with their aqueous solubility and ease of metabolism, as well as their lack of selectivity and systemic adverse reactions, have impeded their use [24, 54]. Novel antioxidant strategies need to improve the therapeutic effect against oxidative stress injury, while limiting adverse effects. Nanoparticles have been proposed as a strategy to fulfill this role. Although classic antioxidants, such as tocopherol, can be readily formulated into micelles [31], and several groups have employed radical-containing nanoparticles [26, 55–61] or encapsulation/conjugation of antioxidants into nanoparticles [62–64], here we focus on the types of nanoparticles with inherent antioxidant and RONS-scavenging properties.

4.1 Ceria NPs

Cerium oxide (CeO_2) nanoparticles, also known as nanoceria or ceria nanoparticles (CNPs), are well-known catalysts that show remarkable pharmacological potential due to their antioxidant properties. This ability is derived from the fraction of Ce^{3+} ions present in CeO_2. In the oxide form of cerium, a lanthanide or rare-earth element, the cerium(IV) and cerium(III) oxidation states coexist. Cerium(IV) is more stable and produces a redox couple responsible for catalytic activity. The reduction in the positive charge by Ce^{3+} is compensated by a corresponding number of oxygen vacancies. The concentration of defects, both Ce^{3+} ions, and oxygen vacancies is greater at the surface of ceria than in the bulk.

Therefore, because of an increase in the surface-to-bulk ratio, nanoceria has a higher surface concentration of Ce^{3+} and enhanced redox activity with respect to larger particles [65]. CNPs scavenge free radicals by reversibly binding oxygen and shifting between the Ce^{3+} (reduced) and Ce^{4+} (oxidized) forms at the particle surface. This ability is comparable to biological antioxidants. Because of this, CNPs are said to exhibit dismutase-mimetic activity [66] and catalase-mimetic activity [67], protecting cells against the two dominant ROS: the superoxide anion and hydrogen peroxide (Fig. 3).

Lee et al. demonstrated that the antioxidant capacity of CNPs is 9-fold higher than that of a benchmark antioxidant [68]. Moreover, the CNPs were reused over 20 times even at high concentrations of hydrogen peroxide. Interestingly, the CNP properties depended on the diameter of the nanocrystals (Figs. 4(a)–4(f)) and the type of surface coating (Fig. 4(g)). The authors found that nanoceria with the smallest size had the greatest antioxidant capacity. Lee et al. attributed it to increased stability of cerium(IV) and higher concentration of cerium(III) on the surface of the nanocrystals, because lattice expansion increases and releases oxygen atoms. As mentioned previously, the type of surface coating of the nanomaterial also significantly affects its antioxidant capacity, which is diminished with thicker polymers. CNPs quench H_2O_2 molecules via a Fenton-like reaction. The antioxidant capacity of ceria depends on cerium(III) concentration and the thickness of the polymer shell. Cerium oxide nanocrystals 3.8 nm in diameter, incorporating 44% cerium(III) and coated with a thin-surface stabilizer (such as poly(acrylic acid) or oleic acid), quench more H_2O_2 than do nanoceria 8.2 nm in diameter, incorporating 30% cerium(III) and covered with thicker polymer (polyethylene imine or polymaleicanhydride-alt-1-octadecene) stabilizers [68].

The catalytic activity of CNPs is also influenced by the surface ratio of Ce^{3+} to Ce^{4+}. The Ce^{3+} sites can remove O_2^- via SOD-mimetics and $^{\bullet}OH$ via redox reactions. However, the Ce^{4+} sites are responsible for the oxidation of H_2O_2 via catalase (CAT)-mimetics [66, 69]. The conversion rate from Ce^{4+} to Ce^{3+} is also crucial because transformation to Ce^{3+} is energetically unfavorable in the auto-conversion process. Adding other dopant ions to ceria nanoparticles can affect the two oxidation states, changing their catalytic performance in scavenging RONS [70]. Soh et al. reported that incorporation of Zr^{4+} ions into CNPs influenced the Ce^{3+}-to-Ce^{4+} ratio and the rate of conversion between the two oxidation states, enhancing the RONS-scavenging capability. This study is further described in section 5.2.

Das et al. [71] demonstrated the antioxidant capacities of CNPs and their ability to protect neuronal cells in a hydrogen peroxide-induced oxidative injury of an adult spinal cord *in vitro* model. Additionally, the authors proposed a schematic mechanistic model illustrating the cyclical regenerative capacity of CNPs in scavenging free radicals from a culture system, as well as the reverse oxidation-state that occurs afterwards; this is shown in Fig. 4(h). The biocompatibility and antioxidant capacity of CNPs have been shown in a wide range of other *in vitro* studies [68, 71–76]. Nanoceria have been shown to scavenge free radicals in murine insulinoma cells treated with hydroquinone [77], prevent retinal degeneration by scavenging RONS in retinal neurons treated with H_2O_2 [78], and protect normal lung fibroblasts from radiation-induced pneumonitis [79].

Among inorganic nanomaterials, ceria NPs are the most widely explored for their antioxidant properties *in vivo* [65, 68, 73, 75, 80–83]. These nanomaterials are used *in vivo* as therapeutic agents in a wide variety of RONS-related diseases. For example, Kim et al. [80] synthesized uniform pegylated ceria nanoparticles of approximately 3.3 nm in size (Figs. 5(a)–5(c)). After several tests *in vitro*, confirming the RONS-scavenging properties of these nanoparticles, they investigated neuroprotective effects in an *in vivo* rat model of induced ischemic stroke. Their results (Figs. 5(d) and 5(e)) demonstrated that there was an optimal dose for obtaining protective benefits using an intravenous injection of the nanoparticles. Low-dose ceria nanoparticles (0.1 and 0.3 $mg \cdot kg^{-1}$) did not decrease infarct volumes, whereas ceria nanoparticles at concentrations of 0.5 and 0.7 $mg \cdot kg^{-1}$ reduced infarct volumes by up to 50% of those of the control group ($p < 0.05$). However, higher doses of ceria nanoparticles (1.0 and 1.5 $mg \cdot kg^{-1}$) failed to show a protective effect against stroke. Microscopic analysis of cell death in frozen brain sections, examined by terminal deoxynucleotidyl transferase-mediated dUTP-biotin nick end labeling (TUNEL) assays, showed that the number of TUNEL-positive cells was markedly decreased in the ceria-injected group. Interestingly, biodistribution studies found that intravenously injected ceria nanoparticles did not sufficiently permeate normal brain tissue, but were able to permeate ischemic brain tissue. This likely occurred because brain ischemia leads to extensive breakage of the blood–brain barrier, which may facilitate passage of the ceria nanoparticles into the brain. Furthermore, lipid peroxide assays have shown that the average concentration of lipid peroxides in the stroke area was 24.6 ± 7.9 μm. However, after treatment with 0.5 $mg \cdot kg^{-1}$ of ceria nanoparticles, the concentration was significantly decreased to 15.5 ± 4.9 μm. This indicates that ceria nanoparticles acted as antioxidants after ischemia.

4.2 Carbon nanomaterials

Fenoglio et al. [84] were the first to describe that carbon nanotubes (CNTs) can be used to scavenge RONS, especially the hydroxyl radical and superoxide anion. CNTs can scavenge a high amount of hydroxyl radicals with consequent decrement of the radical concentration from 1.3 to 0.28 mM. This indicates a scavenging activity of 0.27 $\mu mol \cdot m^{-2}$ for the nanotube surface. The signal from the superoxide radical is also drastically reduced when CNTs are added [84]. This quenching effect is ascribed to reactions occurring at the carbon framework, as occurs with fullerene. Fullerene (C60), another form of crystalline carbon, can act as a radical scavenger. This is because it undergoes a radical addition of carbon-centered radicals due to the high electron affinity of the carbon framework [85–87]. The ability of CNTs to scavenge free radicals is thereby related to fullerene, because CNTs possess a similarly high electron affinity (ca. 2.65 eV). Therefore, both superoxide and hydroxyl radicals may be readily linked at the surface by mechanisms similar to the grafting of organic functionalities [88]. Galano [89] used the density functional theory calculations to model the ability of single-walled carbon nanotubes (SWNTs) to act as free-radical scavengers, and found that once the first radical attached to the nanotube, further additions are increasingly feasible; this indicates that SWNTs can act as free-radical sponges [89].

The RONS-scavenging ability of CNTs, as well as those of other carbon nanomaterials, have been sub-sequently explored for biological applications [90–94]. Huq et al. [91] reported that nontoxic poly(ethylene glycol)-functionalized hydrophilic carbon clusters (PEG-HCCs),

known scavengers of the ROS superoxide ($O_2^{\bullet -}$) and hydroxyl radical, are preferentially internalized by T lymphocytes, more so than by other splenic immune cells. PEG-HCCs can reduce ROS and T lymphocyte-mediated inflammation in delayed-type hypersensitivity and in experimental autoimmune encephalomyelitis (EAE), an animal model of multiple sclerosis. Twenty-four hours after 2 $mg \cdot kg^{-1}$ of PEG-HCCs are subcutaneously injected into the scruff of the neck in rats, PEG-HCCs can scavenge intracellular $O_2^{\bullet -}$ produced via antigen-stimulation of T cells. Consequently, PEG-HCCs reversibly inhibit the production and intracellular levels (approximately 30%) of proinflammatory cytokines (IL-2 and IFN-γ) without showing cytotoxicity. The authors also compared the efficacy of PEG-HCCs to that of vitamin C and trolox (a water-soluble analog of vitamin E), finding that these antioxidants have no effect on T-lymphocyte proliferation; this suggests that PEG-HCCs possess a higher antioxidant capacity than do vitamin C and trolox. In addition, using an active delayed-type hypersensitivity (DTH) inflammation response against ovalbumin in rats, the authors found that a single subcutaneous injection of 2 $mg \cdot kg^{-1}$ PEG-HCCs, at either the time of immunization or challenge, is sufficient to decrease inflammation. In rats with active acute EAE, subcutaneous treatment with 2 $mg \cdot kg^{-1}$ PEG-HCCs every 3 days reduces disease severity and infiltration of immune cells into the central nervous system. Using the same type of carbon nanomaterials, Bitner et al. [95] reported that PEG-HCCs rapidly restore the cerebral blood flow (CBF) in a rat model of mild traumatic brain injury (TBI) when administered during resuscitation; this is a clinically relevant time point for acute circumstances such as stroke. Therapy consisted of tail-vein administration of a single dose of PEG-HCCs (2 $mg \cdot kg^{-1}$) or a diluent vehicle used as a control. After extensive physiological monitoring, results indicated that the nanoparticles can restore cerebral perfusion and normalize the oxidative radical profile. The injection of PEG-HCC antioxidants significantly reduced SO levels in the vasculature and completely restored the levels of vascular NO. This suggests that PEG-HCCs are inherently active therapeutic agents for acute disorders such as stroke, in which reperfusion-based release of RONS is associated with extension and propagation of injury [95].

Lee et al. [92] demonstrated that pretreating rats with amine-modified single-walled carbon nanotubes (a-SWNTs) can protect neurons and enhance the recovery of behavioral functions in rats with induced stroke. The authors injected the nanoparticles into the right lateral ventricle of rats 1 week before inducing ischemic brain injury by middle cerebral artery occlusion (MCAO) surgery. They then assessed the neurological damage. Their results showed that a-SWNT-treated animals had significantly smaller infarct regions than did phosphate buffered saline (PBS)-treated animals 1 day after 90 min of MCAO (Figs. 6(a) and 6(b)). Behavioral evidence of neurological damage was assessed by animal performance on a Rota-Rod treadmill, and by determining the latency times required by the animals to fall from the rotating rod. One day after MCAO, the latency times for both groups were reduced; however, the a-SWNT-treated groups were significantly longer the PBS control (150.6 s versus 114.5 s). This protective effect lasted for up to 7 days, which is indicative of improved motor function and reduced neurological damage (Fig. 6(c)). Inflammation and glial responses are important components of the cellular and molecular pathways involved in stroke-induced destructive processes. The effect of MCAO on inflammation and glial activation in PBS- and a-SWNT-treated rats was determined by immunohistochemical

labeling for glial fibrillary acidic protein (GFAP) and ionized calcium-binding adaptor molecule-1 (Iba-1) in the ipsilateral hemispheres. MCAO increased the expression of both GFAP and Iba-1. However, compared with rats pretreated with PBS, pretreatment with a-SWNT resulted in lower expression of both markers (Figs. 6(d) and 6(e)). The levels of pro-inflammatory cytokines, such as IL-1b and TNF-a, in the ipsilateral cortex were lower in a-SWNT-treated animals than in PBS-injected controls (Figs. 6(f) and 6(g)). This indicates that treatment with a-SWNT protects against ischemia and inhibits glial activation and post-ischemic inflammation. In summary, this study demonstrated that carbon nanotubes can protect the brain from ischemic damage by reducing apoptosis, inflammation, and glial cell activation [92].

4.3 Manganese NPs

Using colorimetric immunoassays, Liu et al. [96] found that manganese dioxide (MnO_2) nanoparticles (MnNPs) possess inherent high peroxidase-, oxidase-, and catalase-like activities; this was further confirmed by several other studies [97–99]. The results of these studies demonstrated that MnO_2 nanoparticles can directly oxidize hydrogen peroxide to produce oxygen and Mn^{2+} according to the following reactions [100]

$$\left.\begin{aligned} 2MnO_2 + H_2O_2 &\rightarrow 2MnOOH + O_2 \\ 2MnOOH + 4H^+ + H_2O_2 &\rightarrow 2Mn^{2+} + 4H_2O + O_2 \\ 2MnOOH + 2H^+ &\rightarrow MnO_2 + Mn^{2+} + 2H_2O \end{aligned}\right| \; MnO_2 + H_2O_2 + 2H^+ \rightarrow Mn^{2+} + O_2 + H_2O$$

Additionally, MnNPs (Mn^{2+}) can mimic the activity of SOD by reacting with $O_2^{\bullet -}$ and producing hydrogen peroxide (final state, Mn^{4+}). Li et al. [97] used the intrinsic enzymatic properties of MnNPs as intelligent cytoprotective shells for individual encapsulation of living cells. The authors evaluated the multienzyme activities of MnNPs alone and attached to yeast cells. The SOD-like activity was estimated using a modified nitro blue tetrazolium (NBT) assay. The results indicated high $O_2^{\bullet -}$ removal capacity, dose-dependent catalytic activity, and an IC50 value of 3.5 $\mu g \cdot mL^{-1}$. The catalaselike activity of these MnO_2 shells was investigated using a terephthalic acid (TA) assay. The results demonstrated that $OH^{\bullet}$ radicals were removed at an efficiency rate of 70%, corresponding to 64 $\mu g \cdot mL^{-1}$. Assessment of H_2O_2 concentration showed that H_2O_2 was decomposed by MnNPs in a dose-dependent manner. The nanozyme shells effectively protected the encased cells from long-term physical and chemical stressors. This protective activity results from the intrinsic multienzyme mimicking activities and high stability of the nanozyme shells [97].

Prasad et al. [101] explored the high reactivity and specificity of MnNPs toward H_2O_2, and the simultaneous and sustained production of O_2. Additionally, they explored how regulating the pH of the tumor microenvironment *in vivo* can improve tumor oxygenation and overcome the hypoxia-associated resistance to radiation therapy. First, the study showed that the NPs could generate O_2 *in vitro* and increase the pH of the medium upon reacting with H_2O_2 and consuming the H^+ ions at endogenous levels (the reaction is described above). Then, the authors assessed the effect of NPs on tumor hypoxia. This was conducted by measuring the levels of hypoxia-inducible factor (HIF)-1α and vascular endothelial growth

factor (VEGF) within orthotopic murine EMT6 tumor-bearing mice after intratumoral (i.t.) injection of an MnNPs suspension. The levels of vascular saturated oxygen (sO_2), before and after the i.t. injections of MnO_2 NPs or saline only (control), were measured using a photoacoustic imaging system. The authors found that sO_2 in tumors treated with MnO_2 NPs increased rapidly by approximately 45% compared with the content in control tumors. After an i.t. injection of NPs labeled with near-infrared dye, the authors observed a substantial diffusion of NPs within the tumor tissue; this occurred almost immediately and was retained within the tumors for at least 24 h (Fig. 7(a)). Pimonidazole was injected into the animals prior to sacrifice; pimonidazole is used to directly detect the presence of hypoxic tumor cells. *Ex vivo* immunohistochemistry showed that tumors treated with MnO_2 NPs for 30 min, 60 min, or 24 h showed 24%, 45%, and 37% less tissue hypoxia, respectively, compared with that of the saline control (Fig. 7(c)). The same tumors also showed a 19%, 21%, and 10% decrease in the expression of HIF-1R and a 7%, 65%, and 65% decrease in the expression of VEGF, after 30 min, 60 min, and 24 h treatment with A-MnO_2 NPs, respectively. Although this was a preliminary study, the authors evaluated whether the NPs can enhance the response to anti-tumoral radiation *in vivo*. This was done by treating tumors in EMT6 tumor-bearing mice with NPs or saline for 30 min prior to irradiation. The average tumor volume in the MnO_2 NPs + radiation therapy (RT) group at day 5 remained at ~ 78 mm^3, while the group treated with RT alone reached an average tumor volume of ~ 231 mm^3 (Fig. 7(d)) [101].

4.4 Other nanomaterials

4.4.1 Platinum nanoparticles (Pt-NPs)—Pt-NPs are also studied for their RONS-scavenging properties; Pt-NPs can act as SOD/catalase mimetics and show activity that is similar to that of the mitochondrial electron transfer complex I [102–104]. Watanabe et al. [104] demonstrated the antioxidant effects of polyacrylic acid (PAA)-protected platinum nanoparticle species (PAA-Pt). In an *in vitro* assessment, PAA-Pt scavenged the $AOO^{\bullet}$, generated by thermal decomposition of AAPH, in a dose-dependent manner. The concentration of NPs at which 50% of $AOO^{\bullet}$ was scavenged (IC_{50}) was 58 ± 4 μM, while controls showed no antioxidant activity. PAA-Pt show scavenging activity that is at least six times more powerful than that of other metal nanoparticles [105]. The inhibitory effects of PAA-Pt on peroxidation of linoleic acid, initiated by $AOO^{\bullet}$, was further assessed by measuring oxygen consumption and thiobarbituric acid reaction substances (TBARS). Oxygen consumption drastically decreased when the NPs were added, but the rate of oxygen consumption did not differ from that of the control. The authors attributed that to the fact that the peroxidation-inhibiting mechanism of PAA-Pt particles may be primarily due to scavenging $LOO^{\bullet}$, which inhibits the propagation of linolate peroxidation. The thiobarbituric acid (TBA) test, designed to assess free MDA produced in lipid peroxidation, indicated that PAA-Pt reduced the production of fatty peroxides by inhibiting the chain propagation of linolate peroxidation initiated by $AOO^{\bullet}$. Pt-NPs have also been applied as RONS scavengers *in vivo*. Katsumi et al. [106] demonstrated for the first time that these NPs prevent hepatic ischemia/reperfusion injury in a mouse model. In their study, two differently-sized Pt-NPs were intravenously injected into mice in which hepatic injury was induced via occluding the portal vein, followed by 6 h reperfusion. The results indicated that both types of NPs accumulated in hepatic non-parenchymal cells post-injection. The smaller Pt-NPs decreased

the activity of plasma alanine aminotransferase (ALT) and aspartate aminotransferase (AST) more than did the larger Pt-NPs. The smaller NPs also effectively reduced the increase in lipid peroxide content (Fig. 8(a)) and suppressed the increase in the ratio of oxidized GSH to reduced glutathione in the ischemic liver.

4.4.2 Melanin nanoparticles (MeNPs)—Previous studies have shown the potential of MeNPs for radical scavenging [107, 108]. However, Liu et al. was the first [109] to show the antioxidant properties of MeNPs in a comprehensive analysis of their scavenging activities against multiple RONS *in vitro* (Figs. 8(b) and 8(c)). Furthermore, Liu et al. demonstrated the feasibility of using those NPs as antioxidant agents *in vivo*. In that study, the antioxidative activity of polyethylene glycol (PEG)-modified MeNPs (PET-MeNPs) toward $O_2^{\bullet -}$ was examined using electron paramagnetic resonance (EPR) spectroscopy and 5-diethoxyphosphoryl-5-methyl-1-pyrroline noxide (DEPMPO) as the producer of radicals. PET-MeNPs reduced the EPR amplitude of DEPMPO-OOH to nearly background levels, indicating that these NPs are robust scavengers of $O_2^{\bullet -}$. Analysis via X-ray photoelectron spectroscopy (XPS) indicated that rather than using a covalent reaction with $O_2^{\bullet -}$, these NPs exhibited a catalytic activity similar to that of SOD. This was ascribed to the radicals in the polymer matrix, which can act as catalytic centers for electron removal from the superoxide. In addition, this antioxidant activity remained unaltered under different pH and even after a 1-year storage at 4 °C. In further experiments, the group verified that MeNPs can also react with $O_2^{\bullet -}$ and form H_2O_2. Thus, the SOD-mimic catalysis of $O_2^{\bullet -}$ can be represented by the reactions

$$\text{melanin}^{\bullet} + O_2^{\bullet -} \rightarrow \text{melanin}^{-} + O_2$$

$$\text{melanin}^{-} + O_2^{\bullet -} + H_2O \rightarrow \text{melanin}^{\bullet} + H_2O_2 + 2OH^{-}$$

In addition, EPR analysis showed that PEG-MeNPs can also scavenge $^{\bullet}OH$, possibly by impeding the Fenton reaction; this is because melanin possesses a strong capability for chelating transition metal ions. Lastly, $^{\bullet}NO$ and $ONOO^{-}$ can be scavenged by nitration and nitrosation of PEG-MeNPs.

4.4.3 Selenium nanoparticles (SeNPs)—Selenium (Se) is part of the antioxidant defense system in the liver and plays an important role in protection against oxidative stress. Many studies have demonstrated that Se supplementation can increase enzyme levels, such as those of GPx, which prevents the accumulation of free radical species, thereby reducing cellular damage [110, 111]. Thus, nanomaterials incorporating selenium have been explored for their intrinsic antioxidant properties. Zhai et al. [112] synthesized SeNPs stabilized using chitosan (CS) (CS-SeNPS) and having different molecular weights; these nanoparticles were then assessed for their antioxidant capacities. Assessments using 2,2-diphenyl-1-picryl-hydrazyl-hydrate (DPPH), 2,2'-azinobis(3-ethylbenzothiazoline-6-sulphonic acid) (ABTS), and lipid peroxide models showed that these CS-SeNPs can scavenge free radicals at different rates (Fig. 8(d)). The scavenging ability of low molecular weight CS-SeNPs (CS(l)-

SeNPs) and high molecular weight CS-SeNPs (CS(h)-SeNPs), shown using ABTS, reached 87.45% ± 7.63% and 89.44% ± 5.03% respectively. *In vitro* cell testing, using BABLC-3T3 or Caco-2, demonstrated that production of intracellular RONS was inhibited in a Se concentration-dependent manner. The topical or oral administration of CS-SeNPs, stabilized with CS(l)-SeNPs, efficiently protected the activity of glutathione peroxidase and prevented lipofuscin formation induced by UV-radiation or d-galactose in mice.

Selenium-doped carbon quantum dots (Se-CQDs) have also been developed for free-radical scavenging (Fig. 8(e)). In a recent study [113], the free radical-scavenging activity of Se-CQDs was assessed with electron spin resonance (ESR) spectroscopy. The results indicated that ESR signals of the diethoxyphosphoryl-5-methyl-l-pyrroline N-oxide (DEMPO)/•OH adduct disappeared when Se-CQDs were added into the solution; this suggests a strong $OH^{\bullet}$ scavenging activity. *In vitro* cellular models also demonstrated that Se-CQDs can protect MDA-MB-231 cells against oxidative stress induced by H_2O_2 treatment. This occurs by reducing H_2O_2-induced cell death and increasing cell viability (as determined by a CCK-8 assay). In addition, quantitative analysis of Rosup-induced RONS generation in MDA-MB-231 cells, assessed via a RONS fluorescence probe (2',7'-dichlorofluorescein diacetate (DCFH-DA)), showed that the fluorescence intensity of DCFH-DA was significantly reduced when Se-CQDs were introduced; this confirms the antioxidant ability of Se-CQDs [113].

5 RONS-related diseases

5.1 Stroke

Acute ischemic cerebrovascular syndrome, commonly known as stroke, is a severe pathology that can result in loss of brain functions, disability, and death. Disruption of the cerebral vascular endothelial cell barrier during stroke leads to local edema caused by increased vascular permeability; this, in turn, can decrease the perfusion of the area. Cerebral reperfusion increases the hazardous effect of early ischemic injury by release of RONS and accumulation of activated neutrophils. This cascade of events is known as reperfusion injury. Via various interrelated mechanisms, excessive RONS play critical roles in the development and progression of endothelial dysfunction, atherogenesis, and cerebral ischemia; this results in brain damage during reperfusion injury [8]. Reoxygenation during reperfusion provides oxygen, which sustains neuronal viability. Oxygen is also required as substrate for the numerous enzymatic oxidation reactions that produce reactive oxidants. In addition, reflow after occlusion often increases the levels of oxygen to those that cannot be utilized by mitochondria under normal physiological flow conditions. Superoxide radicals and H_2O_2 are produced in approximately 2% to 5% of the electron flow in mitochondria isolated from the brain. These constantly produced oxygen radicals are scavenged by SOD, glutathione peroxidase (GSHPx), and catalase. Other antioxidants, including glutathione, ascorbic acid, and vitamin E, are also likely involved in the detoxification of free radicals. During reperfusion, perturbation of antioxidative defense mechanisms results from overproduction of oxygen radicals, inactivation of detoxification systems, consumption of antioxidants, and failure to adequately replenish antioxidants in the ischemic brain tissue [114]. Other sources of RONS include stimulation of the xanthine/xanthine oxidase system

in the cerebral vessels, electron leakage and redox-state alterations of CoQ in the mitochondria, arachidonic acid metabolism, catecholamine oxidation, and activated phagocytes [115]. Ultimately, RONS induce peroxidation of membrane lipids that leads to neuronal and endothelial cell damage and brain edema.

Antioxidants are used as neuroprotective treatment in acute ischemic stroke; more specifically, they are used to prevent ischemic cell death in the infarct-impacted area of the brain and its vicinity. Ebselen, Tirilazad, and Edaravone are drugs that have been clinically tested for stroke. However, only Edaravone was successfully used for stroke management and is in clinical use in Japan. Edaravone (3-methyl-l-phenylpyrazolin-5-one, MCI-186, Radicut®) is a pyrazolin-containing molecule that undergoes keto-enol tautomerization and produces a phenolic structure, generating stable byproducts that do not cause oxidation [17].

In preclinical settings, antioxidant nanoparticles have been used for treating stroke [80, 92, 109]. Liu et al. [109] evaluated the antioxidative and anti-inflammatory activities of PEG-MeNPs *in vivo* using preinjection into the lateral ventricles of ischemic brains in rats (Fig. 9(a)). These *in vivo* studies were conducted after the *in vitro* studies discussed in section 4.4. Rats pretreated with PEG-MeNPs were significantly less vulnerable to ischemia (showing an infarct area of ~ 14%) compared to the saline control group (showing an infarct area of ~ 32% infarct area); the generation of $O_2^{\bullet-}$ was also efficiently suppressed (Figs. 9(b) and 9(d)). The *in vivo* toxicity of the nanoparticles was also assessed via blood and histology analysis after intravenous injection of PEG-MeNPs. The NPs exhibited excellent blood compatibility and did not alter the serum levels of hepatic enzymes, blood urea nitrogen, total protein, or albumin. In addition, no morphological changes or inflammation were found in the different organs analyzed; this indicates that MeNPs can be used as potential RONS scavenger agents in future *in vivo* applications. As mentioned in section 4.1, ceria nanoparticles have also been successfully used to prevent damage resulting from ischemia in the brain [80].

5.2 Sepsis

Experimental and clinical studies have shown that sepsis, a severe systemic inflammatory response to infection, is associated with increased RONS production, depletion of antioxidants, and accumulation of markers of oxidative stress [3]. Studies in pediatric and adult patients with sepsis have shown an increased activity of xanthine oxidase (XO) leading to increased production of RONS [116] and decreased plasma concentrations of common antioxidants such as glutathione, ascorbate, vitamin A, and α-tocopherol. This culminates in an even higher redox imbalance [117]. Indeed, ascorbate plasma concentration is used as a predictive factor for the development of multiple organ failure in patients with sepsis [118]. Diverse molecular mechanisms of inflammation and cellular damage are implicated in the pathogenesis of septic shock and multiple organ failure. These mechanisms include those related to the over-generation of cytokines, eicosanoids, and RONS such as NO, $O_2^{\bullet-}$, and ONOO. In sepsis, there are several potential sources of RONS. These include activation of the phagocytic cells of the immune system (the respiratory burst), production of NO by the vascular endothelium, release of iron and copper ions, metalloproteins, vascular damage caused by ischemia reperfusion, the mitochondrial respiratory electron transport chain,

activation of XO resulting from ischemia and reperfusion, the respiratory burst associated with immune cell activation, and arachidonic acid metabolism [119]. In addition, the sepsis-induced organ dysfunction may be at least partly caused by the mitochondrial dysfunction, which results from oxidative stress and concludes with failure to produce energy. Septic animal hearts display reduced activity of the mitochondrial electron transport chain enzyme complexes [120]. The increased mitochondrial production of $O_2^{\bullet}$ and NO [121], combined with depleted intramitochondrial antioxidants, may severely inhibit oxidative phosphorylation and ATP generation during sepsis [122]. This acquired defect in oxidative phosphorylation prevents cells from using molecular oxygen for ATP production and potentially causes sepsis-induced organ dysfunction [9, 123].

Thus, RONS are among the critical targets in the prevention of sepsis, because the generation of a copious amount of RONS during sepsis is a major cause of multi-organ failure. Therapeutic supplementation with antioxidants, such as selenium, zinc, vitamins, glutathione, melatonin, and α-lipoic acid, has been proposed for the treatment of patients with sepsis [124]. Nanoparticle-based antioxidant therapy has also been proposed for these patients. Soh et al. [81] used ceria-zirconia nanoparticles (CZNPs), of approximately 2 nm in size (Figs. 10(a) and 10(b)), as therapeutic nanomedical agents in models of *in vitro* inflammation and *in vivo* sepsis. For the *in vivo* studies, two different sepsis models were used. One was the lipopolysaccharide (LPS)-induced rat model of endotoxemia; LPS is a major activator of the innate immune system during bacterial infections. The other was the cecal ligation and puncture (CLP)-induced mouse model of bacteremia, which reproduces the main features of secondary bacterial peritonitis; the symptoms include polymicrobial infection and hyperdynamic circulation, which result in sepsis. The results of using the first model showed markedly reduced inflammation in the lungs, less severe sinusoidal dilatation and hepatocyte congestion, and increased survival in the CZNP-treated group compared to that of the control group. Using the CLP-induced mouse model indicated that CZNPs accumulated in the abdominal area and could easily infiltrate the damaged tissues and diffuse through vessels with increased permeability (Fig. 10(e)). Compared with the values of the control, the nanoparticle (NP)-treated group showed lower numbers of CD68(+) macrophages in the cecum and stomach, and reduced inflammatory changes such as mononuclear cell infiltration, mucosal disruption, and exudates with ulcer detritus in the cecum, stomach, and small intestine (Fig. 10(d)). In addition, the median survival rate was extended 2.5 times in the CZNP-treated group compared with that of the control group. This further confirms the therapeutic efficacy of the ceria-zirconia nanoparticles (Fig. 10(c)) [81].

5.3 Neurodegenerative diseases

The term “neurodegenerative” is used to describe a group of diseases characterized by slow progression of neuronal loss. This includes heterogeneous pathologies such as Alzheimer’s disease (AD), Parkinson’s disease (PD), Huntington disease (HD), and amyotrophic lateral sclerosis (ALS). The brain is a highly metabolically active organ. Therefore, it is particularly vulnerable to oxidative stress because of its high demand for oxygen and relatively high levels of redox-active metals, such as iron or copper, which act as catalyzers in the formation of RONS. Additionally, the high levels of polyunsaturated fatty acids in brain-cell membranes render the brain more susceptible to lipid peroxidation [12]. The oxidative

damage caused by RONS is implicated in the pathogenesis of neurodegenerative diseases. For example, mitochondrial dysfunction and enhanced apoptosis, accompanied by poor antioxidant status, are mechanisms implicated in the pathogenesis of AD [125]. The accumulation of RONS may be involved in AD pathogenesis via several mechanisms: (i) Neuronal lesions may activate microglia, which then generate excessive superoxide radicals [126]; (ii) oxidative stress may be involved because the brain physiologically has a low antioxidant potential; and (iii) higher oxidative susceptibility of glial cells and neurons because they are under high metabolic demand and possess a post-mitotic nature [127].

RONS-mediated oxidative DNA damage is one of the prominent features in PD, which is characterized by selective loss of dopaminergic neurons in the substantia nigra. Although the exact mechanism remains unclear, several findings have shown the correlation between oxidative stress and PD. These include: (i) reduced activity of complex I of the respiratory chain in SNc, with consequent generation of excessive RONS; (ii) genetic mutations in several proteins (parkin, α-synuclein, phosphatase, and tensin homolog-induced putative kinase) causing mitochondrial dysfunction [128]; (iii) enhanced dopamine metabolism that leads to accumulation of toxic radicals such as hydroxyl [129]; (iv) accumulation of iron in its redox-active form in the neurons, which increases iron-induced lipid peroxidation [125]; and (v) low levels of the antioxidant enzyme glutathione peroxidase, with consequent accumulation of hydroxyl radicals [130]. ALS and HD are also correlated with an imbalance of RONS [125, 131–134]. Although initial studies on the efficacy of antioxidants in animal models have been promising, the majority of clinical trials in humans have shown negative results with respect to using antioxidants to treat neurodegenerative diseases. Kim et al. have recently reviewed the therapeutic clinical data [12].

As an alternative strategy, RONS-scavenging nanoparticles have been proposed as therapeutic agents. Kwon et al. [135] designed triphenylphosphonium-conjugated ceria nanoparticles (TPP-CNPs) (Fig. 11(a)) that localized to the mitochondria and suppressed neuronal death in the *in vivo* 5FXAD mouse model. This model has a pathology that is similar to that observed in patients with AD, including extensive death of neuronal cells and increased accumulation of Aβ plaques in the subiculum. The NPs were stereotactically injected into the subicula of 5XFAD mice. After 2 months, brain slices stained with NeuN were used to confirm that NPs significantly restored neuronal viability. NP-treated 5XFAD mice showed significantly lower expression of astrocyte and microglia inflammatory markers (Fig. 11(b)). The accumulation of mitochondrial ROS in U373 astrocytes, induced by Aβ-plaques, was also ameliorated by treatment with TPP-CNPs. The authors conclude that the NPs mitigated brain inflammation by reducing the levels of mitochondrial ROS. The 5XFAD mice injected with TPP-CNPs showed normal cristae structures and healthy mitochondrial morphology compared with the severe cristae disruptions and vacuolar cellular shape observed in the subicula of the control group. The RONS-scavenging properties of the NPs were also examined by western blotting, which showed that the level of the oxidative stress marker 4-hydroxynonenal (4-HNE) was significantly decreased after NP administration (Fig. 11(c)). This implies that the NPs can effectively reduce oxidative stress signaling in the mitochondria.

5.4 Diabetes

Oxidative stress and chronic inflammation are implicated in the development of metabolic diseases. This includes diabetes mellitus, a group of physiological dysfunctions characterized by hyperglycemia resulting directly from insulin resistance, inadequate insulin secretion, or excessive secretion of glucagon [136]. Hyperglycemia is a hallmark of both non-insulin-dependent (type 2) and insulin-dependent (type 1) diabetes mellitus. Elevated glucose levels are associated with increased production of RONS by several different mechanisms [137]. For example, a process of glucose auto-oxidation, which is associated with the formation of glycated proteins in the plasma of diabetic patients, can generate superoxide radicals [138]. High glucose levels in the blood can cause increased production of RONS at the mitochondrial complex II [139]. In addition, mitochondrial impairment is implicated in different types of leukocytes and tissues such as the liver, lung, skeletal muscle, spleen, and heart in type 2 diabetes. This confirms the relationship between diabetes and mitochondrial dysfunction, which consequently leads to an imbalance in RONS production [140]. Oxidative stress is the most important factor in the progression of diabetic complications such as nephropathy [141], acute renal failure, retinopathy, and neuropathy [142]. The molecular mechanisms of RONS production and oxidative stress in diabetes have been reviewed previously [143]. Iannitti and Palmieri [18] reviewed the antioxidant therapeutics used for the treatment of diabetic patients. They conclude that Probucol® and Atorvastatin® have been clinically shown to reduce systemic oxidative stress. Moreover, Probucol® may be more clinically useful in patients with strong oxidative stress.

Several nanoparticles with intrinsic antioxidant properties have been used as therapeutic agents for the treatment of diabetes [144–146]. Jahani et al. [144], examined the effect of ceria NPs on diabetic nephropathy, induced by a single intraperitoneal injection of streptozotocin, in a well-established mouse model of diabetes. Mice were treated with nanoceria (60 $mg \cdot kg^{-1}$), vitamin E, or not treated for 4 weeks after injection with streptozotocin. The effects of the treatments were evaluated by measuring the levels of oxidative stress markers and analyzing samples of kidney tissue. This study showed that the NPs prevented the elevation of blood urea nitrogen and creatinine, which are indicators of kidney damage; this action was similar to that of vitamin E. RONS formation in kidney tissue was also markedly decreased in mice that received the NPs but not in those treated with vitamin E. The NPs also inhibited lipid peroxidation, increased the levels of GSH, and decreased catalase activity more efficiently than did vitamin E. Furthermore, the NPs decreased the levels of protein carbonyl (an indicator of protein oxidation) and morphological alterations in the kidney; this shows a decrease in the pathological and biochemical markers of kidney damage in diabetic mice.

Selenium nanoparticles have been investigated for their protective and antioxidative effects in streptozotocin (STZ)-induced diabetic rats [146]. To synthesize SeNPs, sodium selenite was reduced with glutathione in the presence of bovine serum albumin (BSA), resulting in NPs of approximately 19 nm in size [147]. In the treatment groups, diabetic rats received SeNPs (0.1 $mg \cdot kg^{-1}$) orally once a day for 28 days. The authors observed that the activities of testicular GPx, CAT, and SOD were significantly inhibited in STZ-diabetic rats. However, SeNPs restored the activity of these antioxidant enzymes and reduced the levels of lipid

peroxidation and nitric oxide (Figs. 12(a)–12(c)). Diabetic rats were also used to show that a high level of blood glucose (298 $mg{\cdot}d^{-1}{\cdot}L^{-1}$) caused alterations in the normal histological architecture of the testes compared with that of the control rats. Treatment with SeNPs restored the normal morphological structure of the testes (Figs. 12(d)(1)–12(d)(6)). Furthermore, treating STZ-diabetic rats with SeNPs led to an elevation in the expression of the gene *PCNA* (proliferating cell nuclear antigen), which was used to assess spermatogenesis. Dkhil et al. concluded that SeNPs significantly improved diabetes-caused testicular dysfunctions by decreasing oxidative stress and apoptosis. The results indicate that the colloidally stable oleic acid coated.

5.5 Inflammatory diseases

Inflammation is associated with many diseases including atherosclerosis, asthma, cystic fibrosis, and rheumatoid arthritis. Ample evidence suggests that production of free radicals at the site of inflammation may contribute to the pathogenesis of these diseases [137]. Rheumatoid arthritis (RA) is a systemic autoimmune disease characterized by chronic joint inflammation with infiltration of macrophages and activated T cells. Abnormal expression of several adhesion molecules has been shown in RA. This is induced by redox-sensitive signaling pathways, resulting in the migration of monocytes and lymphocytes into the synovium of patients with RA [148]. Atherosclerosis, a disease characterized by hardening and thickening of the arterial wall, is increasingly considered an inflammatory disease. This is because the recruiting, expanding, and sustaining of the monocyte/macrophage population is facilitated during the course of atherosclerosis. This results from the expression of factors, such as adhesion molecules and chemotactic proteins, by endothelial cells [149]. Oxidative stress induces the expression of protein kinases, such as focal adhesion kinase, and intercellular adhesion molecules, such as ICAM-1, leading to the invasion of monocytes, macrophages, and smooth muscle cells [137]. These cell types have the ability to bind to oxidized low-density lipoprotein (LDL), which activates monocytes and macrophages, stimulates the expression of Mn-SOD, and increases the concentration of hydrogen peroxide [150]. This higher accumulation of RONS is hypothesized to provoke a massive macrophage apoptosis, which contributes to the formation of atherosclerotic lesions [151]. Oxidative stress-mediated atherosclerosis has been thoroughly reviewed recently [152].

Wan et al. [153] designed a multicomponent system comprised of a photosensitizer (chlorophyll a; Chla), an electron donor (L-ascorbic acid; AA), and a catalyst of H_2 production (gold nanoparticles; AuNPs); these were encapsulated in a liposomal (Lip) system used as a photodriven nanoreactor (NR) to generate H_2 gas locally. H_2 reduces $^{\bullet}OH$ to H_2O, selectively scavenging the free radical, while preserving other essential RONS for normal signaling regulation. The mechanism driving this system (Fig. 13(a)) depends on laser irradiation and is based on Chla containing a hydrophilic porphyrin ring of greenish pigments, which is excited following photon absorption and generates an electron–hole pair. The hole in the excited Chla* can accept a new electron from AA, returning to its ground state. Colloidal AuNPs (Figs. 13(b)–13(d)) are used as catalysts, which collect the electrons released from the excited Chla* and the protons from the oxidized AA, promoting their conversion to H_2 gas (Fig. 13(e)). The feasibility of using photodriven nanoreactor + laser irradiation (NR+Laser) to mitigate oxidative stress in inflamed tissues was investigated using

a mouse model with LPS-induced paw inflammation and measured using a luminescent probe detected through an *in vivo* imaging system (IVIS) system. The intensity of luminescence, emitted from the inflamed tissue treated with NR+Laser, was significantly reduced compared with that of the control (Fig. 13(f)). Treatment with NR+Laser significantly reduced the LPS-induced increase in the levels of IL-6 and IL-1β; these levels were reduced below those obtained using treatment with bulk solution+laser irradiation (BS +Laser) ($p < 0.05$). This trend was confirmed by histological assessment, in which a reduced infiltration of inflammatory cells was found in the tissues of treated mice.

5.6 Cancer

Oxidative stress-mediated signaling events affect the behavior of cancer cells. In cancer, RONS are involved in cell-cycle progression, as well as the proliferation, survival, apoptosis, energy metabolism, morphology, adhesion, and motility of cancer cells; RONS are also implicated in angiogenesis and maintenance of tumor stemness [14]. Interestingly, RONS have a dual role in cancer. On one hand, RONS can promote protumorigenic signaling, helping cancer cells proliferate, survive, and adapt to hypoxia. Indeed, to hyperactivate protumorigenic signaling events, cancer cells increase their rate of RONS production by acquiring oncogenic mutations, losing tumor suppressors, increasing their metabolism, and adapting to hypoxia (i.e., low oxygen levels). However, RONS can also promote antitumorigenic signaling and trigger the oxidative stress-induced death of cancer cells. To prevent the buildup of RONS and maintain redox balance, cancer cells increase their antioxidant capacity [154]. This review focuses on the applications of nanoparticles with intrinsic RONS-scavenging properties, and not nanoparticles able to generate ROS; Therefore, in this section we discuss how ROS can promote tumorigenesis, and how antioxidant nanoparticles can be used to prevent this process.

RONS can promote protumorigenic signaling via hyperactivation of the PI3K/Akt/mTOR survival pathway, and by oxidizing and inactivating the phosphatases PTEN and PTP1B, the negative regulators of PI3K/Akt signaling. Oncogenic activation of Akt can increase RONS production, which further promotes the survival and proliferation of cancer cells [154]. Several other correlations between ROS and cancer have been found. RONS promote the survival of tumor cells via activation of NF-κB and NRF2 (the transcription factors that upregulate the expression of antioxidants), thus enabling cancer cells to evade RONS-mediated cell death [155]. The complete disruption of the mitochondrial respiratory chain, which reduces the production of RONS, has been shown to diminish tumorigenesis [156]. As a response to hypoxic and glucose-deprived environment, cancer cells undergo metabolic changes, such as HIF stabilization and activation of the 5’ AMP-activated protein kinase (AMPK) and one-carbon metabolic pathways. This enhances the production of NADPH and RONS, and promotes tumor angiogenesis and metastasis [157]. A hypoxic microenvironment also contributes to RONS formation through the release of superoxide, hydrogen peroxide, and hydroxyl radical from the mitochondrial electron transport chain. RONS then stabilize HIF-1α under both normoxic and hypoxic conditions [158]. RONS can play important roles in cancer metastasis by activating matrix metalloproteinases, which degrade components of the extracellular matrix, thereby facilitating the intravasation and extravasation of cancer cells [159]. This activates pathways that stimulate the formation of

invadopodia, the actin-rich membrane protrusions of cancer cells, which facilitate pericellular proteolysis and invasive behavior [160]. RONS can also confer cancer cells with resistance to anoikis, a matrix detachment-induced apoptosis; this occurs via oxidation and activation of Src, leading to constitutive, ligand-independent activation of epidermal growth factor receptor (EGFR) and pro-survival signaling [161]. Further roles of ROS in cancer have been reviewed previously [14, 154, 162].

Antioxidant supplementation has been proposed for patients with cancer. Dietary supplements, such as vitamin C, E, and A, and selenium, have been used in clinical trials. However, most data were inconclusive, with the majority of these compounds showing no protection or exhibiting harmful side effects in the patient cohort. Enzyme-related antioxidants, such as GSH, N-acetylcysteine (NAC), and SOD, as well as NADPH oxidase (NOX) inhibitors, have also been considered. Similarly, clinical trial results have been largely disappointing [162]. Nanoparticles with RONS-scavenging potential have been used for cancer-related applications [163–168]. Giri et al. [164] showed that cerium oxide NPs, 3–5 nm in size (Figs. 14(a) and 14(b)), can potentially inhibit ovarian tumor growth and metastasis by attenuating basal levels of oxidative stress, and invasion and migration of ovarian cancer cells. After their *in vitro* results showed that CNPs can reduce the basal levels of oxidative stress, the effect of these CNPs was assessed *in vivo.* This was conducted by intraperitoneally injecting nude mice with A2780 cells, and then treating these mice with CNPs (0.1 $mg \cdot kg^{-1}$), administered intraperitoneally every 3 days during the study period (30 days total). The abdominal circumference (Figs. 14(c) and 14(d)), indicative of tumor burden in the peritoneum, and tumor weight (Fig. 14(e)) in the CNP-treated mice were significantly reduced compared with those in the untreated mice. The diminished tumor growth was accompanied by attenuation in the size and number of metastatic nodules (Fig. 14(f)) in the lungs of this same tumor model (nude mouse model bearing the human A2780 ovarian carcinoma cell line). To determine the mechanism by which CNPs restrict tumor growth, the authors examined microvessel density in treated and untreated tumor tissue. They found a significant reduction in the CNP-treated tumors as assessed by immunolabeling for CD31, a marker of endothelial cells. The authors observed that the NPs inhibited VEGF-induced proliferation, capillary tube formation, and activation of MMP2 in endothelial cells.

Another cancer-related application of ROS-scavenging nanomaterials is the reaction between manganese nanoparticles and hydrogen peroxide; this reaction generates oxygen, which can be used for modulation of the tumor microenvironment and overcoming hypoxia, which is found in tumor tissues [101, 169, 170]. An example of this was previously described in section 4.3 [101].

6 Summary and future perspectives

We described the several types of reactive oxygen and nitrogen species that are commonly produced by human cells. Although RONS have important biological functions in a healthy cell, an imbalance of highly reactive radical species or their precursors leads to oxidative stress. This is implicated in the pathophysiology of numerous disease processes, which we also discussed. We have also shown that several types of inorganic nanoparticles possess intrinsic antioxidant properties and are used as RONS-scavenging agents in various

biological applications. Overall, we agree with Liu et al. [109] stating that an ideal antioxidant nanomaterial should robustly scavenge multiple primary and secondary RONS, sustain antioxidative activity against oxidative damage, be biocompatible, and have facile controllable properties, such as size and surface that can be modified. The choice of the right nanomaterial for each disease remains complex. For every disease presented here, the process of oxidative stress, rather than any specific RONS, is what most impacts the disease outcome. Choosing the appropriate nanomaterial for RONS scavenging should not be based solely on its RONS-specific antioxidant capacity, but more on its biodistribution profile, half-life in the circulation, immunological profile, and other *in vivo* pharmacokinetics. Among nanoparticles, ceria nanoparticles are the most widely used because of their remarkable enzyme-mimetic capability, and ability to reverse and restore their oxidation state. However, a variety of nanomaterials have been developed. Hence, numerous *in vivo* studies, exploring the antioxidant properties of these nanomaterials, should be expected.

Acknowledgments

This work was supported, in part, by the University of Wisconsin-Madison, the National Institutes of Health (No. NIBIB/NCI P30CA014520) and the Brazilian Science without Borders Program (No. SwB-CNPq).

References

1. Commoner B, Townsend J, Pake GE. Free radicals in biological materials. Nature. 1954; 174:689–691. [PubMed: 13213980]
2. Alfadda AA, Sallam RM. Reactive oxygen species in health and disease. J. Biomed. Biotechnol. 2012; 2012:936486. [PubMed: 22927725]
3. Bayir H. Reactive oxygen species. Crit. Care Med. 2005; 33:S498–S501. [PubMed: 16340433]
4. Dhawan V. Reactive oxygen and nitrogen species: General considerations. In: Ganguly NK, Jindal SK, Biswal S, Barnes PJ, Pawankar R, editorsStudies on Respiratory Disorders. Humana Press; New York: 2014. 27–47.
5. McCord JM, Fridovich I. Superoxide dismutase. An enzymic function for erythrocuprein (hemocuprein). J. Biol. Chem. 1969; 244:6049–6055. [PubMed: 5389100]
6. Rhee SG, Woo HA, Kil IS, Bae SH. Peroxiredoxin functions as a peroxidase and a regulator and sensor of local peroxides. J. Biol. Chem. 2012; 287:4403–4410. [PubMed: 22147704]
7. Ray PD, Huang BW, Tsuji Y. Reactive oxygen species (ROS) homeostasis and redox regulation in cellular signaling. Cell. Signal. 2012; 24:981–990. [PubMed: 22286106]
8. Olmez I, Ozyurt H. Reactive oxygen species and ischemic cerebrovascular disease. Neurochem. Int. 2012; 60:208–212. [PubMed: 22122807]
9. Galley HF. Oxidative stress and mitochondrial dysfunction in sepsis. Br. J. Anaesth. 2011; 107:57–64. [PubMed: 21596843]
10. Urakawa H, Katsuki A, Sumida Y, Gabazza EC, Murashima S, Morioka K, Maruyama N, Kitagawa N, Tanaka T, Hori Y, et al. Oxidative stress is associated with adiposity and insulin resistance in men. J. Clin. Endocrinol. Metab. 2003; 88:4673–4676. [PubMed: 14557439]
11. Datla SR, Griendling KK. Reactive oxygen species, NADPH oxidases, and hypertension. Hypertension. 2010; 56:325–330. [PubMed: 20644010]
12. Kim GH, Kim JE, Rhie SJ, Yoon S. The role of oxidative stress in neurodegenerative diseases. Exp. Neurobiol. 2015; 24:325–340. [PubMed: 26713080]
13. Salminen A, Ojala J, Kaarniranta K, Kauppinen A. Mitochondrial dysfunction and oxidative stress activate inflammasomes: Impact on the aging process and age-related diseases. Cell. Mol. Life Sci. 2012; 69:2999–3013. [PubMed: 22446749]
14. Liou GY, Storz P. Reactive oxygen species in cancer. Free Radic. Res. 2010; 44:479–496. [PubMed: 20370557]

15. Hahn SM, Lepinski DL, DeLuca AM, Mitchell JB, Pellmar TC. Neurophysiological consequences of nitroxide antioxidants. Can. J. Physiol. Pharmacol. 1995; 73:399–403. [PubMed: 7648519]
16. Samuni A, Krishna CM, Riesz P, Finkelstein E, Russo A. A novel metal-free low molecular weight superoxide dismutase mimic. J. Biol. Chem. 1988; 263:17921–17924. [PubMed: 2848018]
17. Firuzi O, Miri R, Tavakkoli M, Saso L. Antioxidant therapy: Current status and future prospects. Curr. Med. Chem. 2011; 18:3871–3888. [PubMed: 21824100]
18. Iannitti T, Palmieri B. Antioxidant therapy effectiveness: An up to date. Eur. Rev. Med. Pharmacol. Sci. 2009; 13:245–278. [PubMed: 19694341]
19. Bjelakovic G, Nikolova D, Simonetti RG, Gluud C. Antioxidant supplements for preventing gastrointestinal cancers. Cochrane Database Syst. Rev. 2008; doi: 10.1002/14651858.CD004183.pub3
20. Lirussi F, Azzalini L, Orando S, Orlando R, Angelico F. Antioxidant supplements for non-alcoholic fatty liver disease and/or steatohepatitis. Cochrane Database Syst. Rev. 2007; doi: 10.1002/14651858.CD004996.pub3
21. Orrell RW, Lane RJ, Ross M. A systematic review of antioxidant treatment for amyotrophic lateral sclerosis/motor neuron disease. Amyotroph. Lateral Scler. 2008; 9:195–211. [PubMed: 18608090]
22. Farinotti M, Vacchi L, Simi S, Di Pietrantonj C, Brait L, Filippini G. Dietary interventions for multiple sclerosis. Cochrane Database Syst. Rev. 2012; doi: 10.1002/14651858.CD004192.pub3
23. Shaheen SO, Newson RB, Rayman MP, Wong APL, Tumilty MK, Phillips JM, Potts JF, Kelly FJ, White PT, Burney PGJ. Randomised, double blind, placebo-controlled trial of selenium supplementation in adult asthma. Thorax. 2007; 62:483–490. [PubMed: 17234657]
24. Cochemé HM, Murphy MP. Can antioxidants be effective therapeutics? Curr. Opin. Invest. Drugs. 2010; 11:426–431.
25. Marchioli R, Schweiger C, Levantesi G, Tavazzi L, Valagussa F. Antioxidant vitamins and prevention of cardiovascular disease: Epidemiological and clinical trial data. Lipids. 2001; 36:S53–S63. [PubMed: 11837994]
26. Chonpathompikunlert P, Fan CH, Ozaki Y, Yoshitomi T, Yeh CK, Nagasaki Y. Redox nanoparticle treatment protects against neurological deficit in focused ultrasound-induced intracerebral hemorrhage. Nanomedicine. 2012; 7:1029–1043. [PubMed: 22394184]
27. Nash KM, Ahmed S. Nanomedicine in the ROS-mediated pathophysiology: Applications and clinical advances. Nanomedicine. 2015; 11:2033–2040. [PubMed: 26255114]
28. Ozcan A, Ogun M. Basic Principles and Clinical Significance of Oxidative Stress. InTech; Rijeka: 2015. Biochemistry of reactive oxygen and nitrogen species.
29. Murphy MP. How mitochondria produce reactive oxygen species. Biochem. J. 2009; 417:1–13. [PubMed: 19061483]
30. Fridovich I. Superoxide dismutases. An adaptation to a paramagnetic gas. J. Biol. Chem. 1989; 264:7761–7764. [PubMed: 2542241]
31. Fukuzawa K, Gebicki JM. Oxidation of α-tocopherol in micelles and liposomes by the hydroxyl, perhydroxyl, and superoxide free radicals. Arch. Biochem. Biophys. 1983; 226:242–251. [PubMed: 6314899]
32. Sheng YW, Abreu IA, Cabelli DE, Maroney MJ, Miller AF, Teixeira M, Valentine JS. Superoxide dismutases and superoxide reductases. Chem. Rev. 2014; 114:3854–3918. [PubMed: 24684599]
33. Winterbourn CC. Reconciling the chemistry and biology of reactive oxygen species. Nat. Chem. Biol. 2008; 4:278–286. [PubMed: 18421291]
34. Rhee SG, Yang KS, Kang SW, Woo HA, Chang TS. Controlled elimination of intracellular H_2O_2: Regulation of peroxiredoxin, catalase, and glutathione peroxidase via post-translational modification. Antioxid. Redox Signal. 2005; 7:619–626. [PubMed: 15890005]
35. Pastor N, Weinstein H, Jamison E, Brenowitz M. A detailed interpretation of OH radical footprints in a TBP-DNA complex reveals the role of dynamics in the mechanism of sequence-specific binding. J. Mol. Biol. 2000; 304:55–68. [PubMed: 11071810]
36. Halliwell B. Oxidants and human-disease: Some new concepts. FASEB J. 1987; 1:358–364. [PubMed: 2824268]

37. Kehrer JP. The Haber–Weiss reaction and mechanisms of toxicity. Toxicology. 2000; 149:43–50. [PubMed: 10963860]
38. Buonocore G, Perrone S, Tataranno ML. Oxygen toxicity: Chemistry and biology of reactive oxygen species. Semin. Fetal Neonatal Med. 2010; 15:186–190. [PubMed: 20494636]
39. Augusto O, Miyamoto S. Oxygen radicals and related species. In: Pantopoulos K, Schipper HM, editorsPrinciples of Free Radical Biomedicine. Nova Science Publishers Inc.; 2011. 1–23.
40. Nathan C, Xie QW. Regulation of biosynthesis of nitric oxide. J. Biol. Chem. 1994; 269:13725–13728. [PubMed: 7514592]
41. Martínez MC, Andriantsitohaina R. Reactive nitrogen species: Molecular mechanisms and potential significance in health and disease. Antioxid. Redox Signal. 2009; 11:669–702. [PubMed: 19014277]
42. Patel RP, McAndrew J, Sellak H, White CR, Jo H, Freeman BA, Darley-Usmar VM. Biological aspects of reactive nitrogen species. Biochim. Biophys. Acta. 1999; 1411:385–400. [PubMed: 10320671]
43. De Grey ADJ. $HO_2^{\bullet}$: The forgotten radical. DNA Cell Biol. 2002; 21:251–257. [PubMed: 12042065]
44. Pullar JM, Vissers MCM, Winterbourn CC. Living with a killer: The effects of hypochlorous acid on mammalian cells. IUBMB Life. 2000; 50:259–266. [PubMed: 11327319]
45. Lee J, Koo N, Min DB. Reactive oxygen species, aging, and antioxidative nutraceuticals. Compr. Rev. Food Sci. F. 2004; 3:21–33.
46. Bartosz G. Reactive oxygen species: Destroyers or messengers? Biochem. Pharmacol. 2009; 77:1303–1315. [PubMed: 19071092]
47. Sharma P, Jha AB, Dubey RS, Pessarakli M. Reactive oxygen species, oxidative damage, and antioxidative defense mechanism in plants under stressful conditions. J. Bot. 2012; 2012 Article ID 217037.
48. Birben E, Sahiner UM, Sackesen C, Erzurum S, Kalayci O. Oxidative stress and antioxidant defense. World Allergy Organ. J. 2012; 5:9–19. [PubMed: 23268465]
49. Dizdaroglu M, Jaruga P, Birincioglu M, Rodriguez H. Free radical-induced damage to DNA: Mechanisms and measurement. Free Radic. Biol. Med. 2002; 32:1102–1115. [PubMed: 12031895]
50. Phaniendra A, Jestadi DB, Periyasamy L. Free radicals: Properties, sources, targets, and their implication in various diseases. Indian J. Clin. Biochem. 2015; 30:11–26. [PubMed: 25646037]
51. Dean RT, Fu S, Stocker R, Davies MJ. Biochemistry and pathology of radical-mediated protein oxidation. Biochem. J. 1997; 324:1–18. [PubMed: 9164834]
52. Butterfield DA, Koppal T, Howard B, Subramaniam R, Hall N, Hensley K, Yatin S, Allen K, Aksenov M, Aksenova M, et al. Structural and functional changes in proteins induced by free radical-mediated oxidative stress and protective action of the antioxidants N-tert-butyl-α-phenylnitrone and vitamin Ea. Ann. N Y Acad. Sci. 1998; 854:448–462. [PubMed: 9928452]
53. Chevion M, Berenshtein E, Stadtman ER. Human studies related to protein oxidation: Protein carbonyl content as a marker of damage. Free Radical Res. 2000; 33:S99–S108. [PubMed: 11191280]
54. Shimizu M, Yoshitomi T, Nagasaki Y. The behavior of ROS-scavenging nanoparticles in blood. J. Clin. Biochem. Nutr. 2014; 54:166–173. [PubMed: 24895479]
55. Yoshitomi T, Hirayama A, Nagasaki Y. The ROS scavenging and renal protective effects of pH-responsive nitroxide radical-containing nanoparticles. Biomaterials. 2011; 32:8021–8028. [PubMed: 21816462]
56. Nagasaki Y. Nitroxide radicals and nanoparticles: A partnership for nanomedicine radical delivery. Ther. Deliv. 2012; 3:165–179. [PubMed: 22834195]
57. Vong LB, Kobayashi M, Nagasaki Y. Evaluation of the toxicity and antioxidant activity of redox nanoparticles in zebrafish (*Danio rerio*) embryos. Mol. Pharm. 2016; 13:3091–3097. [PubMed: 27186993]
58. Yue CX, Yang YM, Zhang CL, Alfranca G, Cheng SL, Ma LJ, Liu YL, Zhi X, Ni J, Jiang WH, et al. ROS-responsive mitochondria-targeting blended nanoparticles: Chemo- and photodynamic synergistic therapy for lung cancer with on-demand drug release upon irradiation with a single light source. Theranostics. 2016; 6:2352–2366. [PubMed: 27877240]

59. Yoshitomi T, Nagasaki Y. Nitroxyl radical-containing nanoparticles for novel nanomedicine against oxidative stress injury. Nanomedicine. 2011; 6:509–518. [PubMed: 21542688]
60. Vong LB, Tomita T, Yoshitomi T, Matsui H, Nagasaki Y. An orally administered redox nanoparticle that accumulates in the colonic mucosa and reduces colitis in mice. Gastroenterology. 2012; 143:1027–1036. [PubMed: 22771506]
61. Marushima A, Suzuki K, Nagasaki Y, Yoshitomi T, Toh K, Tsurushima H, Hirayama A, Matsumura A. Newly synthesized radical-containing nanoparticles enhance neuroprotection after cerebral ischemia-reperfusion injury. Neurosurgery. 2011; 68:1418–1426. [PubMed: 21273921]
62. Kalmodia S, Vandhana S, Tejaswini Rama BR, Jayashree B, Sreenivasan Seethalakshmi T, Umashankar V, Yang WR, Barrow CJ, Krishnakumar S, Elchuri SV. Bioconjugation of antioxidant peptide on surface-modified gold nanoparticles: A novel approach to enhance the radical scavenging property in cancer cell. Cancer Nanotechnol. 2016; 7:1. [PubMed: 26900409]
63. Li JC, Zhang J, Chen Y, Kawazoe N, Chen GP. TEMPO-conjugated gold nanoparticles for reactive oxygen species scavenging and regulation of stem cell differentiation. ACS Appl. Mater. Interfaces. 2017; 9:35683–35692. [PubMed: 28944661]
64. Pu HL, Chiang WL, Maiti B, Liao ZX, Ho YC, Shim MS, Chuang EY, Xia YN, Sung HW. Nanoparticles with dual responses to oxidative stress and reduced pH for drug release and anti-inflammatory applications. ACS Nano. 2014; 8:1213–1221. [PubMed: 24386907]
65. Celardo I, Pedersen JZ, Traversa E, Ghibelli L. Pharmacological potential of cerium oxide nanoparticles. Nanoscale. 2011; 3:1411–1420. [PubMed: 21369578]
66. Korsvik C, Patil S, Seal S, Self WT. Superoxide dismutase mimetic properties exhibited by vacancy engineered ceria nanoparticles. Chem. Commun. 2007:1056–1058.
67. Singh S, Dosani T, Karakoti AS, Kumar A, Seal S, Self WT. A phosphate-dependent shift in redox state of cerium oxide nanoparticles and its effects on catalytic properties. Biomaterials. 2011; 32:6745–6753. [PubMed: 21704369]
68. Lee SS, Song WS, Cho M, Puppala HL, Nguyen P, Zhu HG, Segatori L, Colvin VL. Antioxidant properties of cerium oxide nanocrystals as a function of nanocrystal diameter and surface coating. ACS Nano. 2013; 7:9693–9703. [PubMed: 24079896]
69. Pirmohamed T, Dowding JM, Singh S, Wasserman B, Heckert E, Karakoti AS, King JES, Seal S, Self WT. Nanoceria exhibit redox state-dependent catalase mimetic activity. Chem. Commun. 2010; 46:2736–2738.
70. Migani A, Vayssilov GN, Bromley ST, Illas F, Neyman KM. Dramatic reduction of the oxygen vacancy formation energy in ceria particles: A possible key to their remarkable reactivity at the nanoscale. J. Mater. Chem. 2010; 20:10535–10546.
71. Das M, Patil S, Bhargava N, Kang JF, Riedel LM, Seal S, Hickman JJ. Auto-catalytic ceria nanoparticles offer neuroprotection to adult rat spinal cord neurons. Biomaterials. 2007; 28:1918–1925. [PubMed: 17222903]
72. Perez JM, Asati A, Nath S, Kaittanis C. Synthesis of biocompatible dextran-coated nanoceria with pH-dependent antioxidant properties. Small. 2008; 4:552–556. [PubMed: 18433077]
73. Niu JL, Azfer A, Rogers LM, Wang XH, Kolattukudy PE. Cardioprotective effects of cerium oxide nanoparticles in a transgenic murine model of cardiomyopathy. Cardiovasc. Res. 2007; 73:549–559. [PubMed: 17207782]
74. Mandoli C, Pagliari F, Pagliari S, Forte G, Di Nardo P, Licoccia S, Traversa E. Stem cell aligned growth induced by CeO_2 nanoparticles in PLGA scaffolds with improved bioactivity for regenerative medicine. Adv. Funct. Mater. 2010; 20:1617–1624.
75. Hirst SM, Karakoti AS, Tyler RD, Sriranganathan N, Seal S, Reilly CM. Anti-inflammatory properties of cerium oxide nanoparticles. Small. 2009; 5:2848–2856. [PubMed: 19802857]
76. Karakoti A, Singh S, Dowding JM, Seal S, Self WT. Redox-active radical scavenging nanomaterials. Chem. Soc. Rev. 2010; 39:4422–4432. [PubMed: 20717560]
77. Tsai YY, Oca-Cossio J, Agering K, Simpson NE, Atkinson MA, Wasserfall CH, Constantinidis I, Sigmund W. Novel synthesis of cerium oxide nanoparticles for free radical scavenging. Nanomedicine. 2007; 2:325–332. [PubMed: 17716177]
78. Chen JP, Patil S, Seal S, McGinnis JF. Rare earth nanoparticles prevent retinal degeneration induced by intracellular peroxides. Nat. Nanotechnol. 2006; 1:142–150. [PubMed: 18654167]

79. Colon J, Herrera L, Smith J, Patil S, Komanski C, Kupelian P, Seal S, Jenkins DW, Baker CH. Protection from radiation-induced pneumonitis using cerium oxide nanoparticles. Nanomedicine. 2009; 5:225–231. [PubMed: 19285453]
80. Kim CK, Kim T, Choi IY, Soh M, Kim D, Kim YJ, Jang H, Yang HS, Kim JY, Park HK, et al. Ceria nanoparticles that can protect against ischemic stroke. Angew. Chem., Int. Ed. 2012; 51:11039–11043.
81. Soh M, Kang DW, Jeong HG, Kim D, Kim DY, Yang W, Song C, Baik S, Choi IY, Ki SK, et al. Ceria-zirconia nanoparticles as an enhanced multi-antioxidant for sepsis treatment. Angew. Chem., Int. Ed. 2017; 56:11399–11403.
82. Kang DW, Kim CK, Jeong HG, Soh M, Kim T, Choi IY, Ki SK, Kim DY, Yang W, Hyeon T, et al. Biocompatible custom ceria nanoparticles against reactive oxygen species resolve acute inflammatory reaction after intracerebral hemorrhage. Nano Res. 2017; 10:2743–2760.
83. Wu HB, Li FY, Wang SF, Lu JX, Li JQ, Du Y, Sun XL, Chen XY, Gao JQ, Ling DS. Ceria nanocrystals decorated mesoporous silica nanoparticle based ROS-scavenging tissue adhesive for highly efficient regenerative wound healing. Biomaterials. 2018; 151:66–77. [PubMed: 29078200]
84. Fenoglio I, Tomatis M, Lison D, Muller J, Fonseca A, Nagy JB, Fubini B. Reactivity of carbon nanotubes: Free radical generation or scavenging activity? Free Radic. Biol. Med. 2006; 40:1227–1233. [PubMed: 16545691]
85. Krusic PJ, Wasserman E, Keizer PN, Morton JR, Preston KF. Radical reactions of C_{60}. Science. 1991; 254:1183–1185. [PubMed: 17776407]
86. Morton JR, Preston KF, Krusic PJ, Hill SA, Wasserman E. ESR studies of the reaction of alkyl radicals with fullerene C_{60}. J. Phys. Chem. 1992; 96:3576–3578.
87. Lin AMY, Chyi BY, Wang SD, Yu HH, Kanakamma PP, Luh TY, Chou CK, Ho LT. Carboxyfullerene prevents iron-induced oxidative stress in rat brain. J. Neurochem. 1999; 72:1634–1640. [PubMed: 10098871]
88. Ying YM, Saini RK, Liang F, Sadana AK, Billups WE. Functionalization of carbon nanotubes by free radicals. Org. Lett. 2003; 5:1471–1473. [PubMed: 12713301]
89. Galano A. Carbon nanotubes as free-radical scavengers. J. Phys. Chem. C. 2008; 112:8922–8927.
90. Lucente-Schultz RM, Moore VC, Leonard AD, Price BK, Kosynkin DV, Lu M, Partha R, Conyers JL, Tour JM. Antioxidant single-walled carbon nanotubes. J. Am. Chem. Soc. 2009; 131:3934–3941. [PubMed: 19243186]
91. Huq R, Samuel ELG, Sikkema WKA, Nilewski LG, Lee T, Tanner MR, Khan FS, Porter PC, Tajhya RB, Patel RS, et al. Preferential uptake of antioxidant carbon nanoparticles by T lymphocytes for immunomodulation. Sci. Rep. 2016; 6:33808. [PubMed: 27654170]
92. Lee HJ, Park J, Yoon OJ, Kim HW, Lee DY, Kim DH, Lee WB, Lee NE, Bonventre JV, Kim SS. Amine-modified single-walled carbon nanotubes protect neurons from injury in a rat stroke model. Nat. Nanotechnol. 2011; 6:121–125. [PubMed: 21278749]
93. Yudoh K, Karasawa R, Masuko K, Kato T. Water-soluble fullerene (C60) inhibits the development of arthritis in the rat model of arthritis. Int. J. Nanomedicine. 2009; 4:217–225. [PubMed: 19918368]
94. Huang ST, Ho CS, Lin CM, Fang HW, Peng YX. Development and biological evaluation of C_{60} fulleropyrrolidine-thalidomide dyad as a new anti-inflammation agent. Bioorg. Med. Chem. 2008; 16:8619–8626. [PubMed: 18723357]
95. Bitner BR, Marcano DC, Berlin JM, Fabian RH, Cherian L, Culver JC, Dickinson ME, Robertson CS, Pautler RG, Kent TA, et al. Antioxidant carbon particles improve cerebrovascular dysfunction following traumatic brain injury. ACS Nano. 2012; 6:8007–8014. [PubMed: 22866916]
96. Liu X, Wang Q, Zhao HH, Zhang LC, Su YY, Lv Y. BSA-templated MnO_2 nanoparticles as both peroxidase and oxidase mimics. Analyst. 2012; 137:4552–4558. [PubMed: 22900262]
97. Li W, Liu Z, Liu CQ, Guan YJ, Ren JS, Qu XG. Manganese dioxide nanozymes as responsive cytoprotective shells for individual living cell encapsulation. Angew. Chem., Int. Ed. 2017; 56:13661–13665.
98. Huang YY, Liu Z, Liu CQ, Ju EG, Zhang Y, Ren JS, Qu XG. Self-assembly of multi-nanozymes to mimic an intracellular antioxidant defense system. Angew. Chem., Int. Ed. 2016; 55:6646–6650.

99. Wan Y, Qi P, Zhang D, Wu JJ, Wang Y. Manganese oxide nanowire-mediated enzyme-linked immunosorbent assay. Biosens. Bioelectron. 2012; 33:69–74. [PubMed: 22326701]
100. Luo XL, Xu JJ, Zhao W, Chen HY. A novel glucose ENFET based on the special reactivity of MnO_2 nanoparticles. Biosens. Biolectron. 2004; 19:1295–1300.
101. Prasad P, Gordijo CR, Abbasi AZ, Maeda A, Ip A, Rauth AM, DaCosta RS, Wu XY. Multifunctional albumin-MnO_2 nanoparticles modulate solid tumor microenvironment by attenuating hypoxia, acidosis, vascular endothelial growth factor and enhance radiation response. ACS Nano. 2014; 8:3202–3212. [PubMed: 24702320]
102. Hikosaka K, Kim J, Kajita M, Kanayama A, Miyamoto Y. Platinum nanoparticles have an activity similar to mitochondrial NADH: Ubiquinone oxidoreductase. Colloids Surf. B. Biointerfaces. 2008; 66:195–200. [PubMed: 18653320]
103. Tabata S, Nishida H, Masaki Y, Tabata K. Stoichiometric photocatalytic decomposition of pure water in Pt/TiO_2 aqueous suspension system. Catal. Lett. 1995; 34:245–249.
104. Watanabe A, Kajita M, Kim J, Kanayama A, Takahashi K, Mashino T, Miyamoto Y. *In vitro* free radical scavenging activity of platinum nanoparticles. Nanotechnology. 2009; 20:455105. [PubMed: 19834242]
105. Huang B, Zhang JS, Hou JW, Chen C. Free radical scavenging efficiency of Nano-Se *in vitro*. Free Radic. Biol. Med. 2003; 35:805–813. [PubMed: 14583345]
106. Katsumi H, Fukui K, Sato K, Maruyama S, Yamashita S, Mizumoto E, Kusamori K, Oyama M, Sano M, Sakane T, et al. Pharmacokinetics and preventive effects of platinum nanoparticles as reactive oxygen species scavengers on hepatic ischemia/reperfusion injury in mice. Metallomics. 2014; 6:1050–1056. [PubMed: 24658875]
107. Ju KY, Lee Y, Lee S, Park SB, Lee JK. Bioinspired polymerization of dopamine to generate melanin-like nanoparticles having an excellent free-radical-scavenging property. Biomacromolecules. 2011; 12:625–632. [PubMed: 21319809]
108. Panzella L, Gentile G, D'Errico G, Della Vecchia NF, Errico ME, Napolitano A, Carfagna C, d'Ischia M. Atypical structural and π-electron features of a melanin polymer that lead to superior free-radical-scavenging properties. Angew. Chem., Int. Ed. 2013; 52:12684–12687.
109. Liu YL, Ai KL, Ji XY, Askhatova D, Du R, Lu LH, Shi JJ. Comprehensive insights into the multi-antioxidative mechanisms of melanin nanoparticles and their application to protect brain from injury in ischemic stroke. J. Am. Chem. Soc. 2017; 139:856–862. [PubMed: 27997170]
110. Tapiero H, Townsend DM, Tew KD. The antioxidant role of selenium and seleno-compounds. Biomed. Pharmacother. 2003; 57:134–144. [PubMed: 12818475]
111. Qin SY, Huang BX, Ma JF, Wang X, Zhang JB, Li LH, Chen F. Effects of selenium-chitosan on blood selenium concentration, antioxidation status, and cellular and humoral immunity in mice. Biol. Trace Elem. Res. 2015; 165:145–152. [PubMed: 25634140]
112. Zhai XN, Zhang CY, Zhao GH, Stoll S, Ren FZ, Leng XJ. Antioxidant capacities of the selenium nanoparticles stabilized by chitosan. J. Nanobiotechnology. 2017; 15:4. [PubMed: 28056992]
113. Li F, Li TY, Sun CX, Xia JH, Jiao Y, Xu HP. Selenium-doped carbon quantum dots for free-radical scavenging. Angew. Chem., Int. Ed. 2017; 56:9910–9914.
114. Chan PH. Role of oxidants in ischemic brain damage. Stroke. 1996; 27:1124–1129. [PubMed: 8650725]
115. Alexandrova ML, Bochev PG, Markova VI, Bechev BG, Popova MA, Danovska MP, Simeonova VK. Oxidative stress in the chronic phase after stroke. Redox Rep. 2003; 8:169–176. [PubMed: 12935315]
116. Galley HF, Davies MJ, Webster NR. Xanthine oxidase activity and free radical generation in patients with sepsis syndrome. Crit. Care Med. 1996; 24:1649–1653. [PubMed: 8874300]
117. Takeda K, Shimada Y, Amano M, Sakai T, Okada T, Yoshiya I. Plasma lipid peroxides and alpha-tocopherol in critically ill patients. Crit. Care Med. 1984; 12:957–959. [PubMed: 6499481]
118. Borrelli E, Roux-Lombard P, Grau GE, Girardin E, Ricou B, Dayer JM, Suter PM. Plasma concentrations of cytokines, their soluble receptors, and antioxidant vitamins can predict the development of multiple organ failure in patients at risk. Crit. Care Med. 1996; 24:392–397. [PubMed: 8625625]

119. Victor VM, Espulgues JV, Hernández-Mijares A, Rocha M. Oxidative stress and mitochondrial dysfunction in sepsis: A potential therapy with mitochondria-targeted antioxidants. Infect. Disord. Drug Targets. 2009; 9:376–389. [PubMed: 19689380]
120. Levy RJ, Vijayasarathy C, Raj NR, Avadhani NG, Deutschman CS. Competitive and noncompetitive inhibition of myocardial cytochrome C oxidase in sepsis. Shock. 2004; 21:110–114. [PubMed: 14752282]
121. Taylor DE, Ghio AJ, Piantadosi CA. Reactive oxygen species produced by liver mitochondria of rats in sepsis. Arch. Biochem. Biophys. 1995; 316:70–76. [PubMed: 7840680]
122. Brealey D, Brand M, Hargreaves I, Heales S, Land J, Smolenski R, Davies NA, Cooper CE, Singer M. Association between mitochondrial dysfunction and severity and outcome of septic shock. Lancet. 2002; 360:219–223. [PubMed: 12133657]
123. Levy RJ. Mitochondrial dysfunction, bioenergetic impairment, and metabolic down-regulation in sepsis. Shock. 2007; 28:24–28. [PubMed: 17483747]
124. Berger MM, Chioléro RL. Antioxidant supplementation in sepsis and systemic inflammatory response syndrome. Crit. Care Med. 2007; 35:S584–S590. [PubMed: 17713413]
125. Manoharan S, Guillemin GJ, Abiramasundari RS, Essa MM, Akbar M, Akbar MD. The role of reactive oxygen species in the pathogenesis of Alzheimer's disease, Parkinson's disease, and Huntington's disease: A mini review. Oxid. Med. Cell. Longev. 2016; 2016 Article ID 8590578.
126. Nakajima K, Kohsaka S. Microglia: Activation and their significance in the central nervous system. J. Biochem. 2001; 130:169–175. [PubMed: 11481032]
127. Friedman J. Why is the nervous system vulnerable to oxidative stress?. In: Gadoth N, Göbel HH, editorsOxidative Stress and Free Radical Damage in Neurology. Humana Press; Totowa, NJ: 2011. 19–27.
128. Blesa J, Trigo-Damas I, Quiroga-Varela A, Jackson-Lewis VR. Oxidative stress and Parkinson's disease. Front. Neuroanat. 2015; 9:91. [PubMed: 26217195]
129. Gerlach M, Double KL, Ben-Shachar D, Zecca L, Youdim MBH, Riederer P. Neuromelanin and its interaction with iron as a potential risk factor for dopaminergic neurodegeneration underlying Parkinson's disease. Neurotox. Res. 2003; 5:35–43. [PubMed: 12832223]
130. Ihara Y, Chuda M, Kuroda S, Hayabara T. Hydroxyl radical and superoxide dismutase in blood of patients with Parkinson's disease: Relationship to clinical data. J. Neurol. Sci. 1999; 170:90–95. [PubMed: 10561523]
131. Barber SC, Mead RJ, Shaw PJ. Oxidative stress in ALS: A mechanism of neurodegeneration and a therapeutic target. Biochim. Biophys. Acta. 2006; 1762:1051–1067. [PubMed: 16713195]
132. Said Ahmed M, Hung WY, Zu JS, Hockberger P, Siddique T. Increased reactive oxygen species in familial amyotrophic lateral sclerosis with mutations in *SOD1*. J. Neurol. Sci. 2000; 176:88–94. [PubMed: 10930589]
133. Kumar A, Ratan RR. Oxidative stress and Huntington's disease: The good, the bad, and the ugly. J. Huntingtons Dis. 2016; 5:217–237. [PubMed: 27662334]
134. Gil-Mohapel J, Brocardo PS, Christie BR. The role of oxidative stress in Huntington's disease: Are antioxidants good therapeutic candidates? Curr. Drug Targets. 2014; 15:454–468. [PubMed: 24428525]
135. Kwon HJ, Cha MY, Kim D, Kim DK, Soh M, Shin K, Hyeon T, Mook-Jung I. Mitochondria-targeting ceria nanoparticles as antioxidants for Alzheimer's disease. ACS Nano. 2016; 10:2860–2870. [PubMed: 26844592]
136. Blair M. Diabetes mellitus review. Urol. Nurs. 2016; 36:27–36. [PubMed: 27093761]
137. Dröge W. Free radicals in the physiological control of cell function. Physiol. Rev. 2002; 82:47–95. [PubMed: 11773609]
138. Wolff SP, Jiang ZY, Hunt JV. Protein glycation and oxidative stress in diabetes mellitus and ageing. Free Radic. Biol. Med. 1991; 10:339–352. [PubMed: 1855674]
139. Nishikawa T, Edelstein D, Du XL, Yamagishi S, Matsumura T, Kaneda Y, Yorek MA, Beebe D, Oates PJ, Hammes HP, et al. Normalizing mitochondrial superoxide production blocks three pathways of hyperglycaemic damage. Nature. 2000; 404:787–790. [PubMed: 10783895]
140. Di Meo S, Reed TT, Venditti P, Victor VM. Role of ROS and RNS sources in physiological and pathological conditions. Oxid. Med. Cell. Longev. 2016; 2016 Article ID 1245049.

141. Ha H, Kim KH. Pathogenesis of diabetic nephropathy: The role of oxidative stress and protein kinase C. Diabetes Res. Clin. Pract. 1999; 45:147–151. [PubMed: 10588367]
142. Thompson KH, Godin DV. Micronutrients and antioxidants in the progression of diabetes. Nutr. Res. 1995; 15:1377–1410.
143. Newsholme P, Cruzat VF, Keane KN, Carlessi R, de Bittencourt PI Jr. Molecular mechanisms of ROS production and oxidative stress in diabetes. Biochem. J. 2016; 473:4527–4550. [PubMed: 27941030]
144. Jahani M, Shokrzadeh M, Vafaei-Pou Z, Zamani E, Shaki F. Potential role of cerium oxide nanoparticles for attenuation of diabetic nephropathy by inhibition of oxidative damage. Asian J. Anim. Vet. Adv. 2016; 11:226–234.
145. BarathManiKanth S, Kalishwaralal K, Sriram M, Pandian SRK, Youn HS, Eom S, Gurunathan S. Anti-oxidant effect of gold nanoparticles restrains hyperglycemic conditions in diabetic mice. J. Nanobiotechnology. 2010; 8:16. [PubMed: 20630072]
146. Dkhil MA, Zrieq R, Al-Quraishy S, Abdel Moneim AE. Selenium nanoparticles attenuate oxidative stress and testicular damage in streptozotocin-induced diabetic rats. Molecules. 2016; 21:1517.
147. Al-Quraishy S, Dkhil MA, Abdel Moneim AE. Anti-hyperglycemic activity of selenium nanoparticles in streptozotocin-induced diabetic rats. Int. J. Nanomedicine. 2015; 10:6741–6756. [PubMed: 26604749]
148. Valko M, Leibfritz D, Moncol J, Cronin MT, Mazur M, Telser J. Free radicals and antioxidants in normal physiological functions and human disease. Int. J. Biochem. Cell Biol. 2007; 39:44–84. [PubMed: 16978905]
149. Alexander RW. Hypertension and the pathogenesis of atherosclerosis. Hypertension. 1995; 25:155–161. [PubMed: 7843763]
150. Kinscherf R, Deigner HP, Usinger C, Pill J, Wagner M, Kamencic H, Hou D, Chen M, Schmiedt W, Schrader M, et al. Induction of mitochondrial manganese superoxide dismutase in macrophages by oxidized LDL: Its relevance in atherosclerosis of humans and heritable hyperlipidemic rabbits. FASEB J. 1997; 11:1317–1328. [PubMed: 9409551]
151. Kinscherf R, Wagner M, Kamencic H, Bonaterra GA, Hou DM, Schiele RA, Deigner HP, Metz J. Characterization of apoptotic macrophages in atheromatous tissue of humans and heritable hyperlipidemic rabbits. Atherosclerosis. 1999; 144:33–39. [PubMed: 10381275]
152. Yang XY, Li Y, Li YD, Ren XM, Zhang XY, Hu D, Gao YH, Xing YW, Shang HC. Oxidative stress-mediated atherosclerosis: Mechanisms and therapies. Front. Physiol. 2017; 8:600. [PubMed: 28878685]
153. Wan WL, Lin YJ, Chen HL, Huang CC, Shih PC, Bow YR, Chia WT, Sung HW. *In situ* nanoreactor for photosynthesizing H_2 gas to mitigate oxidative stress in tissue inflammation. J. Am. Chem. Soc. 2017; 139:12923–12926. [PubMed: 28870078]
154. Reczek CR, Chandel NS. The two faces of reactive oxygen species in cancer. Annu. Rev. Cancer Biol. 2017; 1:79–98.
155. Morgan MJ, Liu ZG. Crosstalk of reactive oxygen species and NF-κB signaling. Cell Res. 2011; 21:103–115. [PubMed: 21187859]
156. Weinberg F, Hamanaka R, Wheaton WW, Weinberg S, Joseph J, Lopez M, Kalyanaraman B, Mutlu GM, Budinger GRS, Chandel NS. Mitochondrial metabolism and ROS generation are essential for Kras-mediated tumorigenicity. Proc. Natl. Acad. Sci. USA. 2010; 107:8788–8793. [PubMed: 20421486]
157. Ye JB, Fan J, Venneti S, Wan YW, Pawel BR, Zhang J, Finley LWS, Lu C, Lindsten T, Cross JR, et al. Serine catabolism regulates mitochondrial redox control during hypoxia. Cancer Discov. 2014; 4:1406–1417. [PubMed: 25186948]
158. Huang LE, Arany Z, Livingston DM, Bunn HF. Activation of hypoxia-inducible transcription factor depends primarily upon redox-sensitive stabilization of its α subunit. J. Biol. Chem. 1996; 271:32253–32259. [PubMed: 8943284]
159. Nelson KK, Melendez JA. Mitochondrial redox control of matrix metalloproteinases. Free Radic. Biol. Med. 2004; 37:768–784. [PubMed: 15304253]

160. Diaz B, Shani G, Pass I, Anderson D, Quintavalle M, Courtneidge SA. Tks5-dependent, nox-mediated generation of reactive oxygen species is necessary for invadopodia formation. Sci. Signal. 2009; 2:ra53. [PubMed: 19755709]

161. Giannoni E, Fiaschi T, Ramponi G, Chiarugi P. Redox regulation of *anoikis* resistance of metastatic prostate cancer cells: Key role for Src and EGFR-mediated pro-survival signals. Oncogene. 2009; 28:2074–2086. [PubMed: 19377510]

162. Morry J, Ngamcherdtrakul W, Yantasee W. Oxidative stress in cancer and fibrosis: Opportunity for therapeutic intervention with antioxidant compounds, enzymes, and nanoparticles. Redox Biol. 2017; 11:240–253. [PubMed: 28012439]

163. Prylutska S, Grynyuk I, Matyshevska O, Prylutskyy Y, Evstigneev M, Scharff P, Ritter U. C_{60} fullerene as synergistic agent in tumor-inhibitory doxorubicin treatment. Drugs R. D. 2014; 14:333–340. [PubMed: 25504158]

164. Giri S, Karakoti A, Graham RP, Maguire JL, Reilly CM, Seal S, Rattan R, Shridhar V. Nanoceria: A rare-earth nanoparticle as a novel anti-angiogenic therapeutic agent in ovarian cancer. PLoS One. 2013; 8:e54578. [PubMed: 23382918]

165. Vassie JA, Whitelock JM, Lord MS. Endocytosis of cerium oxide nanoparticles and modulation of reactive oxygen species in human ovarian and colon cancer cells. Acta Biomater. 2017; 50:127–141. [PubMed: 27940194]

166. Vassie JA, Whitelock JM, Lord MS. Targeted delivery and redox activity of folic acid-functionalized nanoceria in tumor cells. Mol. Pharm. 2018; 15:994–1004. [PubMed: 29397735]

167. Alili L, Sack M, von Montfort C, Giri S, Das S, Carroll KS, Zanger K, Seal S, Brenneisen P. Downregulation of tumor growth and invasion by redoxactive nanoparticles. Antioxid. Redox Signal. 2013; 19:765–778. [PubMed: 23198807]

168. Hijaz M, Das S, Mert I, Gupta A, Al-Wahab Z, Tebbe C, Dar S, Chhina J, Giri S, Munkarah A, et al. Folic acid tagged nanoceria as a novel therapeutic agent in ovarian cancer. BMC Cancer. 2016; 16:220. [PubMed: 26979107]

169. Lin TS, Zhao XZ, Zhao S, Yu H, Cao WM, Chen W, Wei H, Guo HQ. O_2-generating MnO_2 nanoparticles for enhanced photodynamic therapy of bladder cancer by ameliorating hypoxia. Theranostics. 2018; 8:990–1004. [PubMed: 29463995]

170. Zhu WW, Dong ZL, Fu TT, Liu JJ, Chen Q, Li YG, Zhu R, Xu LG, Liu Z. Modulation of hypoxia in solid tumor microenvironment with MnO_2 nanoparticles to enhance photodynamic therapy. Adv. Funct. Mater. 2016; 26:5490–5498.

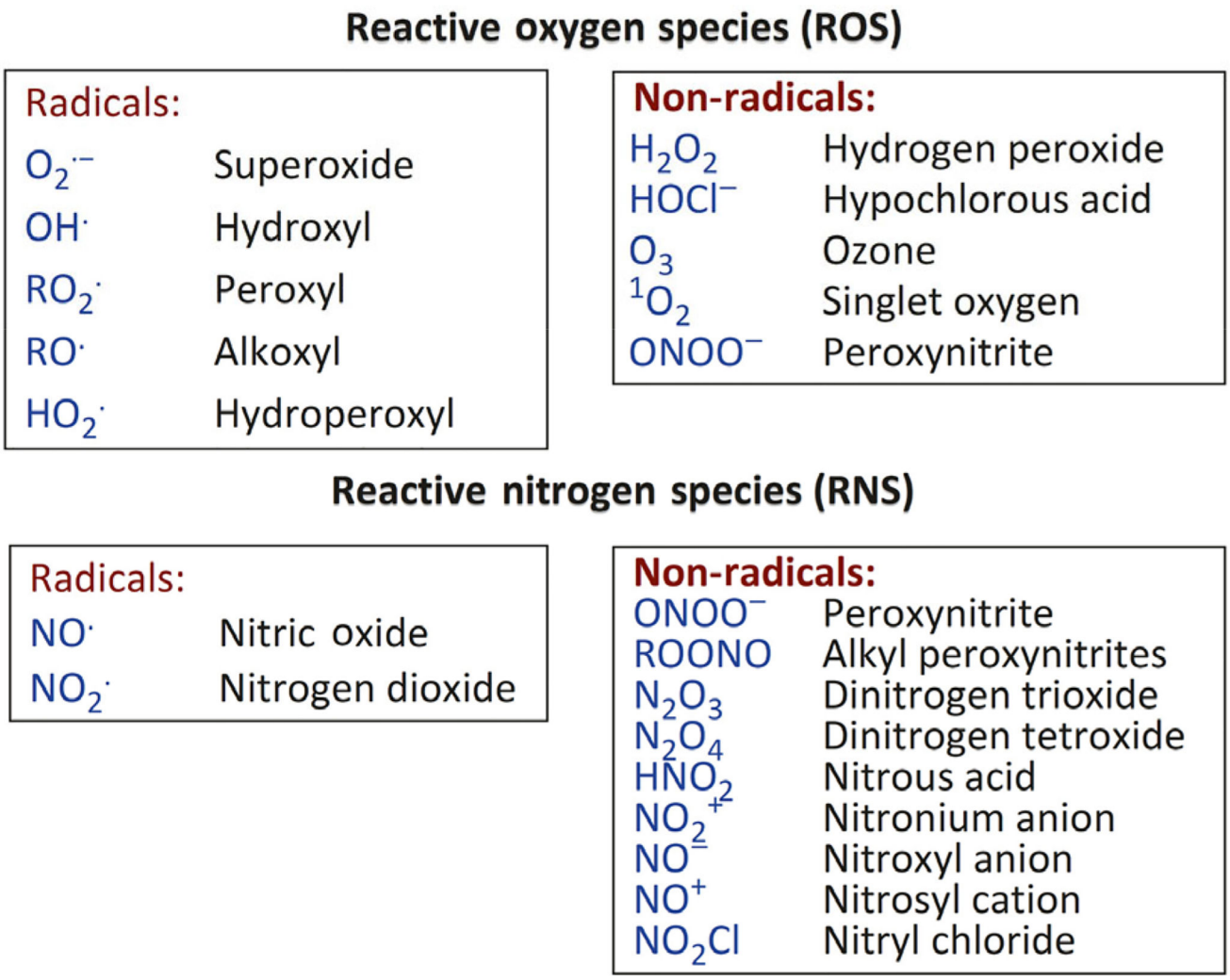

Figure 1.
Types of RONS produced in the cell (reproduced with permission from Ref. [4], © Springer eBook 2014).

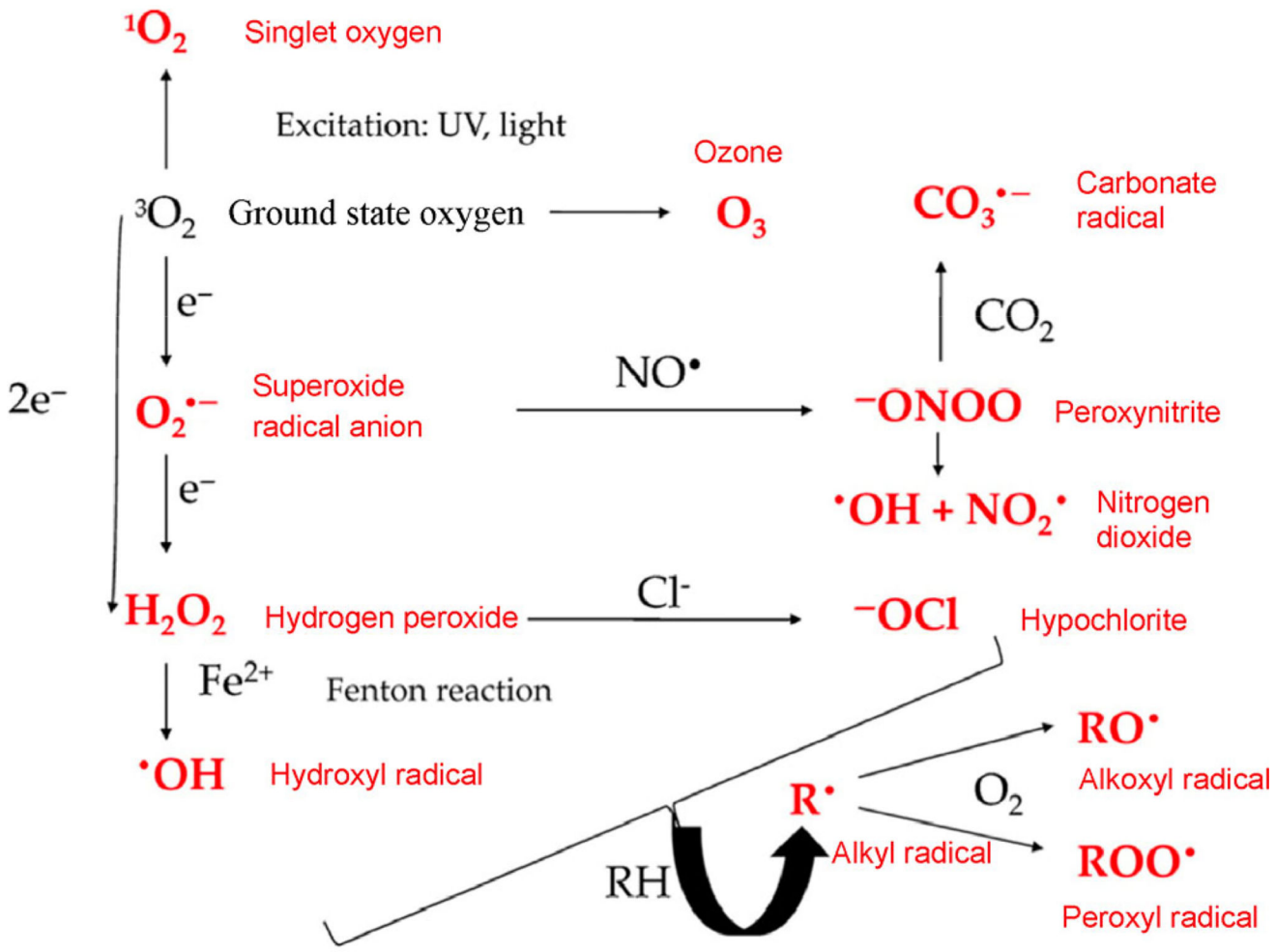

Figure 2.
Main routes of RONS generation; RH=organic molecule (reproduced with permission from Ref. [46], © Elsevier 2009).

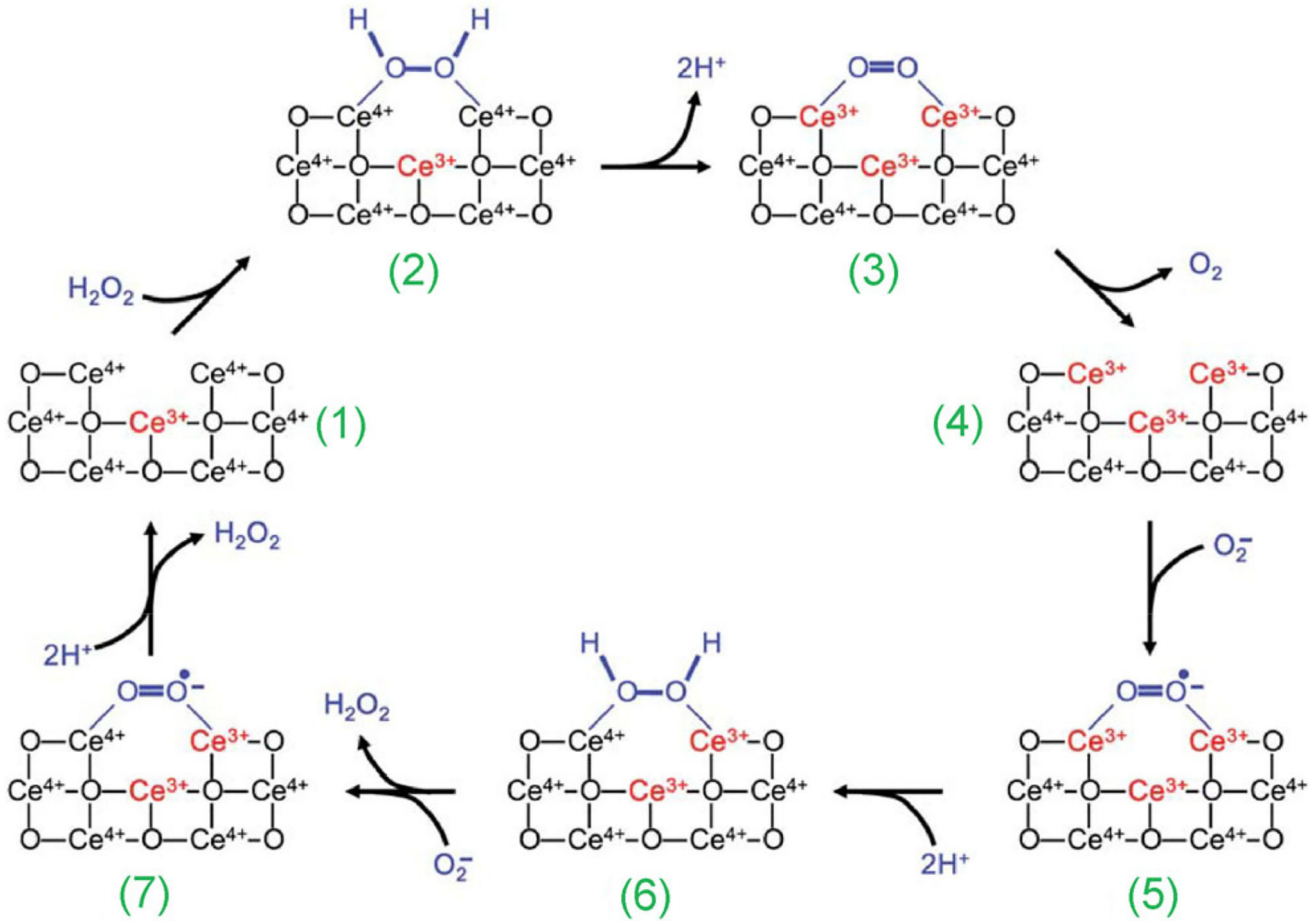

Figure 3.

A model of the reaction mechanism for oxidation of hydrogen peroxide by nanoceria and regeneration via reduction by superoxide. An oxygen vacancy site on nanoceria surface (1) presents a $2Ce^{4+}$ binding site for H_2O_2 (2). After the release of protons and two-electron transfer to the two cerium ions (3), oxygen is released from the now fully reduced oxygen vacancy site (4). Subsequently, superoxide can bind to this site (5); after the transfer of a single electron from one Ce^{3+}, and uptake of two protons from the solution, H_2O_2 is formed (6) and can be released. After repeating this reaction with a second superoxide molecule (7), the oxygen vacancy site returns to the initial $2Ce^{4+}$ state (1). It is also possible that the third Ce^{3+} indicated, which generates the oxygen vacancy, can participate directly in the reaction mechanism. Reproduced with permission from Ref. [65], © Royal Society of Chemistry 2011.

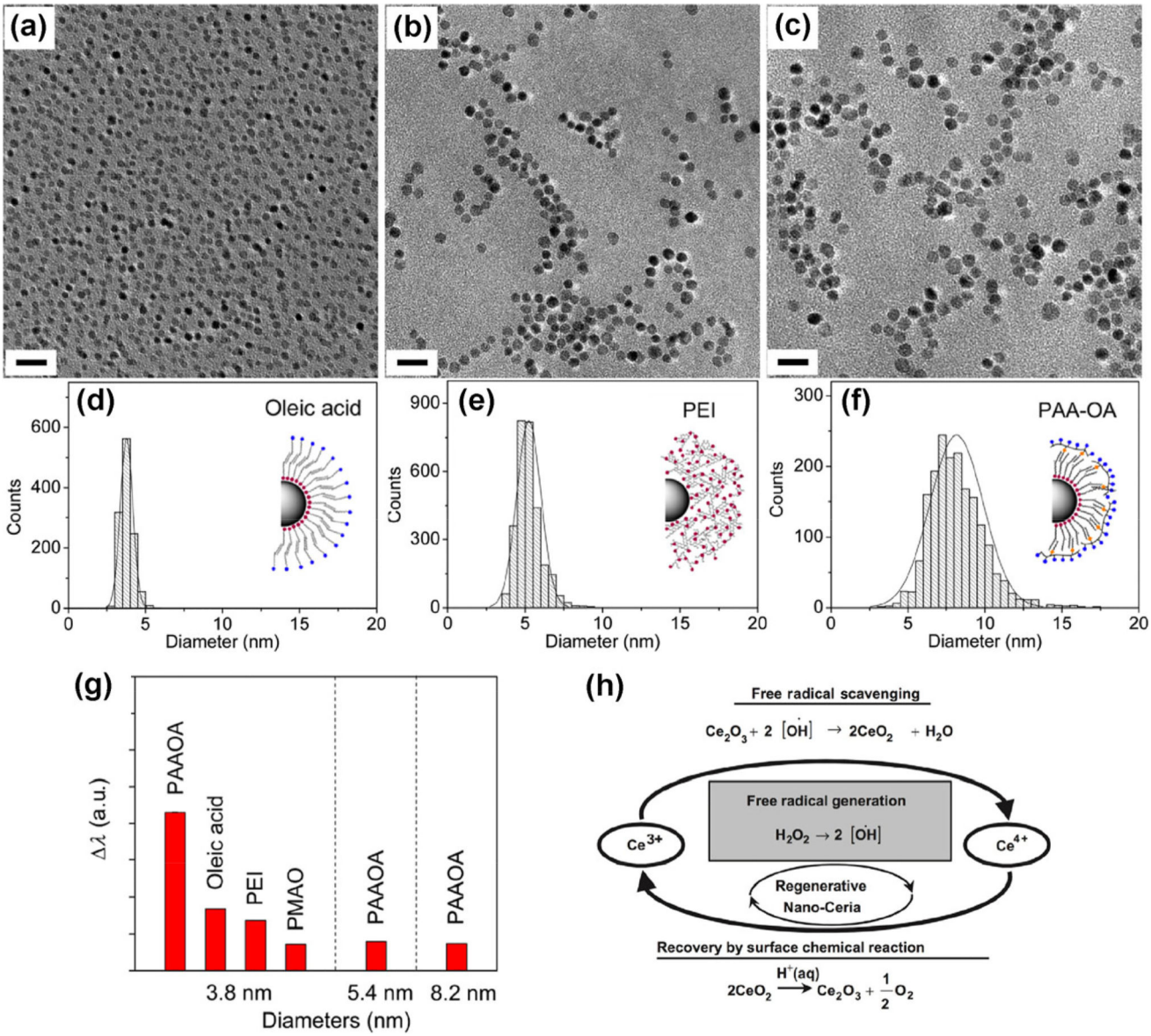

Figure 4.

TEM micrographs (a)–(c) of water-soluble nanoceria. All scale bars are 20 nm from (a) to (c). (a) Oleic acid-coated CeO_2 nanoparticles (3.8 ± 0.4 nm); (b) PEI-coated CeO_2 nanoparticles (5.4 ±1.0 nm); (c) PAAOA-coated CeO_2 nanoparticles (8.2 ± 1.7 nm). The size distribution histograms (d)–(f) are placed at the bottom of the corresponding images together with a schematic depiction of the coated nanomaterial. (g) The extent of H_2O_2 quenching capacity depends on the diameter and surface stabilizers of nanoceria. To compare the surface polymer-dependent H_2O_2 quenching efficiency of nanoceria, the extent of the band shift ($\Delta\lambda$) was measured at 0.30 absorbance after the injection of H_2O_2 from the control. For diameter-dependent H_2O_2 quenching, three CeO_2 suspensions with different diameters were utilized (d = 3.8, 5.4, and 8.2 nm; PAAOA-coated CeO_2). Surface coating-dependent H_2O_2 quenching was shown by 3.8-nm CeO_2 covered with four different polymers (PAAOA, oleic acid, PEI, and PMAO). (h) Schematic detailing of the proposed regenerative properties of

nanoceria, and probable mechanism of free-radical scavenging and auto-catalytic behavior of cerium oxide nanoparticles. (a)–(g) are adapted with permission from Ref. [68], © American Chemical Society 2013. (h) is reproduced with permission from Ref. [71], © Elsevier 2007.

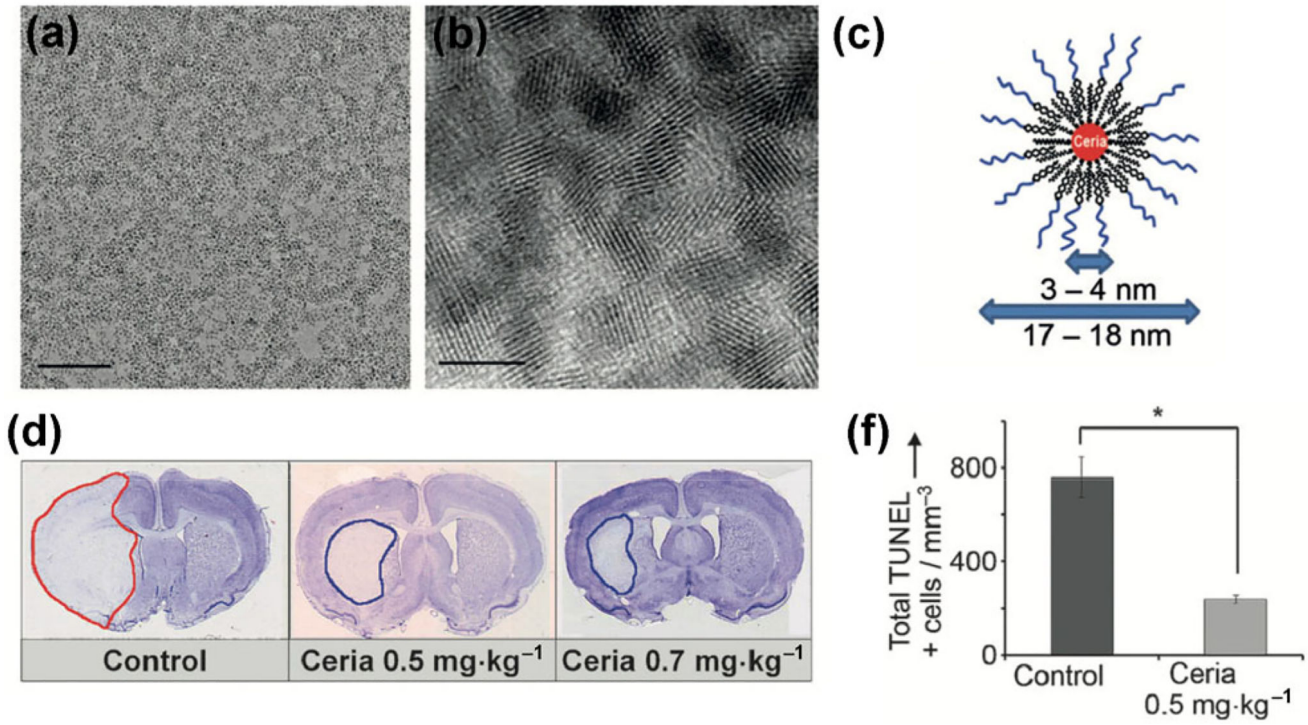

Figure 5.

(a)–(c) Characterization of ceria nanoparticles. (a) TEM images reveal discrete and uniform 3 nm-sized ceria nanoparticles. Scale bar = 100 nm. (b) High-resolution TEM images reveal a cross-lattice pattern, demonstrating the highly crystalline nature of ceria nanoparticles. Scale bar = 5 nm. (c) The geometry of ceria nanoparticles after hydrophilic encapsulation with phospholipid-PEG (core diameter (d_c) = 3–4 nm; hydrodynamic diameter (d_h) = 17–18 nm). (d) and (e) Infarct volume and ischemic cell death *in vivo*. (d) Representative slices showing that 0.5 and 0.7 mg·kg^{-1} of ceria nanoparticles can significantly reduce infarct volumes. (e) The number of TUNEL-positive cells are decreased in the ceriainjected group (*$p < 0.05$; $n = 4$ each). Adapted with permission from Ref. [80], © John Wiley and Sons 2012.

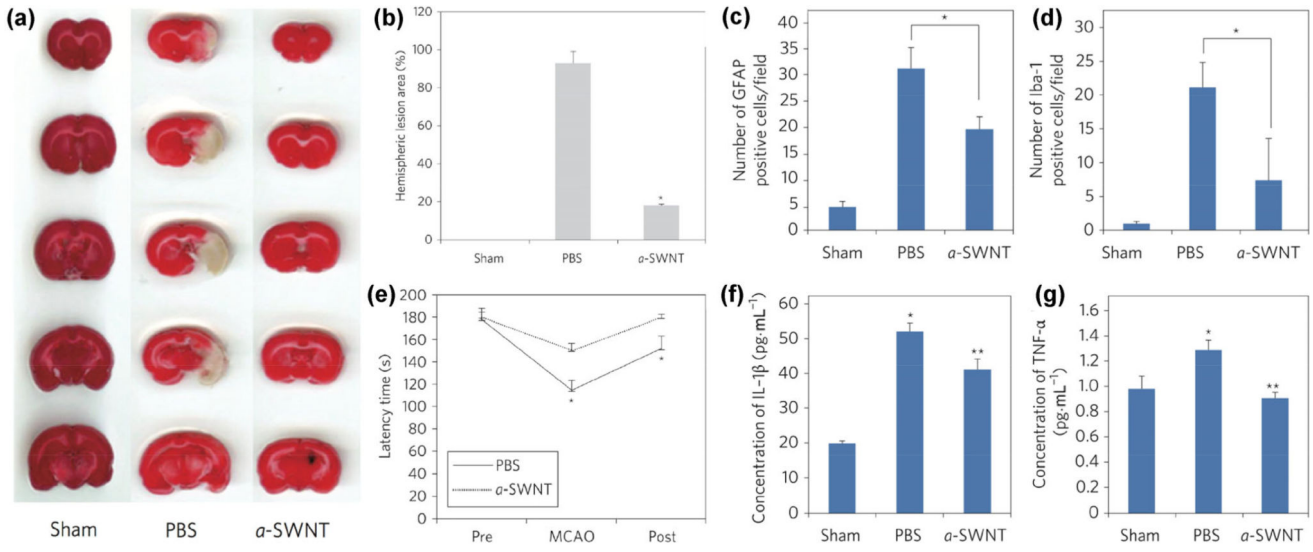

Figure 6.

(a) Coronal brain sections (stained with triphenyltetrazolium chloride (TTC)) of sham-operated control and PBS- or a-SWNT-treated rats. Brain slices were arranged in sequence. White areas represent the infarcted region after MCAO. (b) Quantification of the ischemic lesions of brain sections in (a). (c) and (d) Bar graphs showing quantification of (c) GFAP- and (d) Iba-1-positive cells on the ipsilateral side. Data are the mean number of cells from five random fields. (e) Graph showing that pretreatment with a-SWNTs reduces neurological damage after ischemia. Neurological score was evaluated by the Rota-Rod treadmill test. (f) and (g) Effects of treatment with a-SWNTs on the production of proinflammatory cytokines IL-1b (f) and TNF-a (g). Cytokine levels, determined by ELISA, were normalized against the cortex of the contralateral hemisphere. Immunohistochemical analysis and ELISA were performed 7 days after MCAO. Data are expressed as means ± s.e.m. *$p < 0.001$. Adapted with permission from Ref. [92], © Springer Nature 2011.

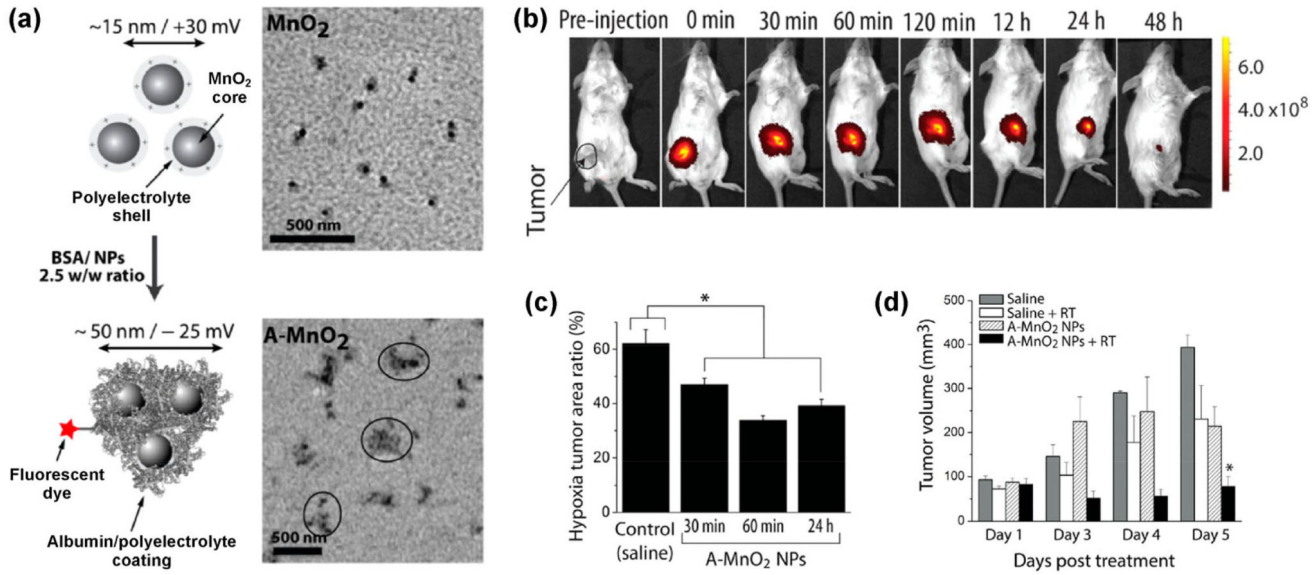

Figure 7.

(a) Diagram and TEM images of MnO_2 and A-MnO_2 NPs. Precursor MnO_2 NPs (~ 15 nm) are stabilized by positively charged PAH. In A-MnO_2 (~ 50 nm), several MnO_2 particles are entrapped in a poly(allylamine hydrochloride) (PHA)/BSA complex due to strong electrostatic interaction between the protein and polymer. (b) Representative optical images of EMT6 tumor-bearing mouse with i.t. injected near-infrared-labeled A-MnO_2 NPs; images were acquired at various times. (c) Quantification of tumor hypoxia after treatments, determined using classified images (not shown) ($n = 3$). Error bars represent standard errors of the mean. (*) Statistically significant difference ($^*p = 6.9 \times 10^{-5}$) as compared to saline (control)-treated group. (d) Tumor volume measured over time after treatment. Adapted with permission from Ref. [101], © American Chemical Society 2014.

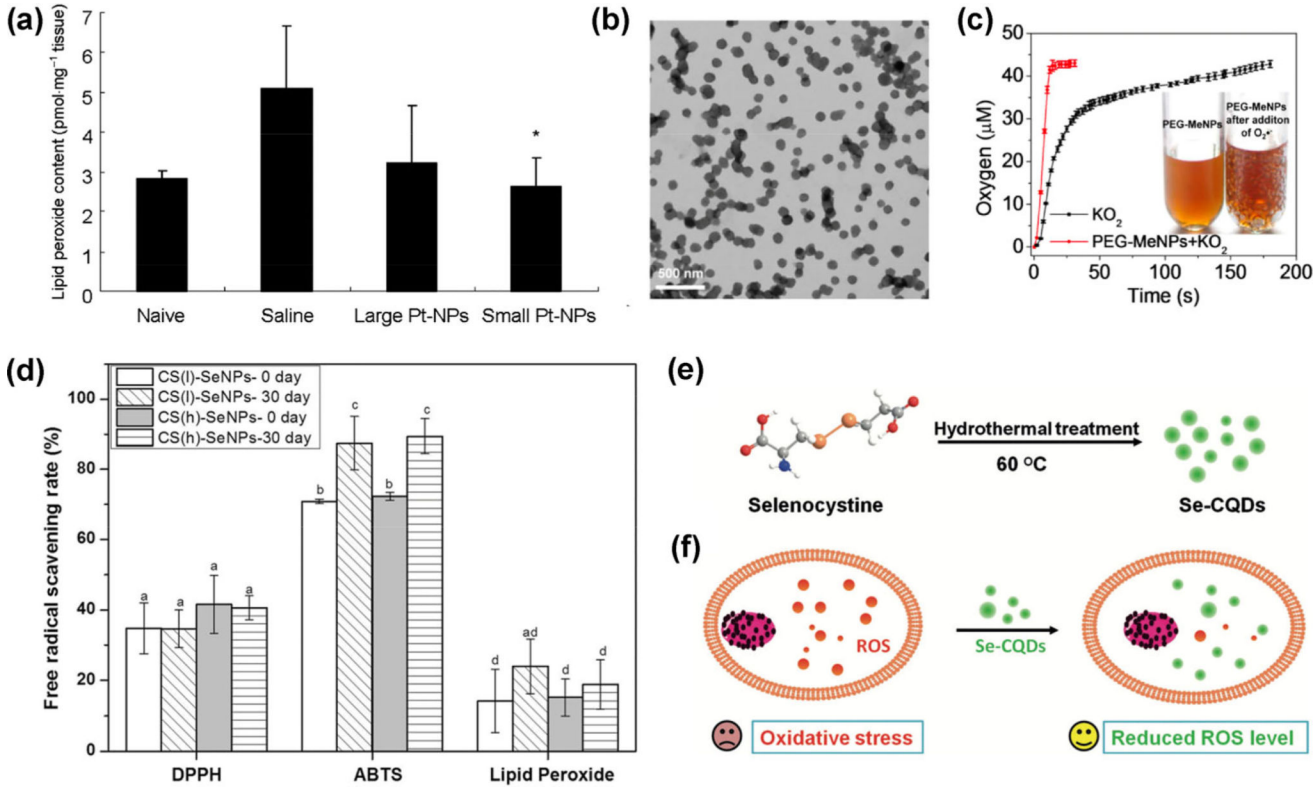

Figure 8.

(a) Platinum nanoparticles [106]—the lipid peroxide content in mouse liver 6 h after hepatic ischemia/reperfusion. Lipid peroxides were detected by TBA method. Each of the Pt-NPs was administered at an equivalent platinum dose (50 mg of platinum per kg). The results are expressed as the mean ± S.D. of 3 to 7 mice. $*p < 0.05$, indicates significant difference from the saline-treated group. (b) and (c) Melanin nanoparticles [109]. (b) TEM image of PEG-MeNPs. (c) O_2 production in the KO_2 solution (100 μM) with or without PEG-MeNPs. The insert is the digital image of the PEG-MeNPs solution before and after the addition of KO_2. (d) Selenium nanoparticles [112]—comparison of the antioxidant capacities of CS-SeNPs in DPPH, ABTS, and lipid peroxidation systems. The different letter markers denote the significant mean difference at $p < 0.05$. (e) and (f) Selenium-doped carbon quantum dots [113]. (e) Synthesis of Se-CQDs with green fluorescence using hydrothermal treatment with selenocysteine. (f) Once the Se-CQDs are internalized in cells with elevated ROS levels, a portion of the ROS can be scavenged, protecting the cells from ROS-induced damage. (a) is reproduced with permission from Ref. [106], © Royal Society of Chemistry 2014. (b) and (c) are reproduced with permission from Ref. [109], © American Chemical Society 2017. (d) is reproduced with permission from Ref. [112] under the Creative Commons Attribution License, © Zhai et al. 2017. (e) and (f) are reproduced with permission from Ref. [113], © John Wiley and Sons 2017.

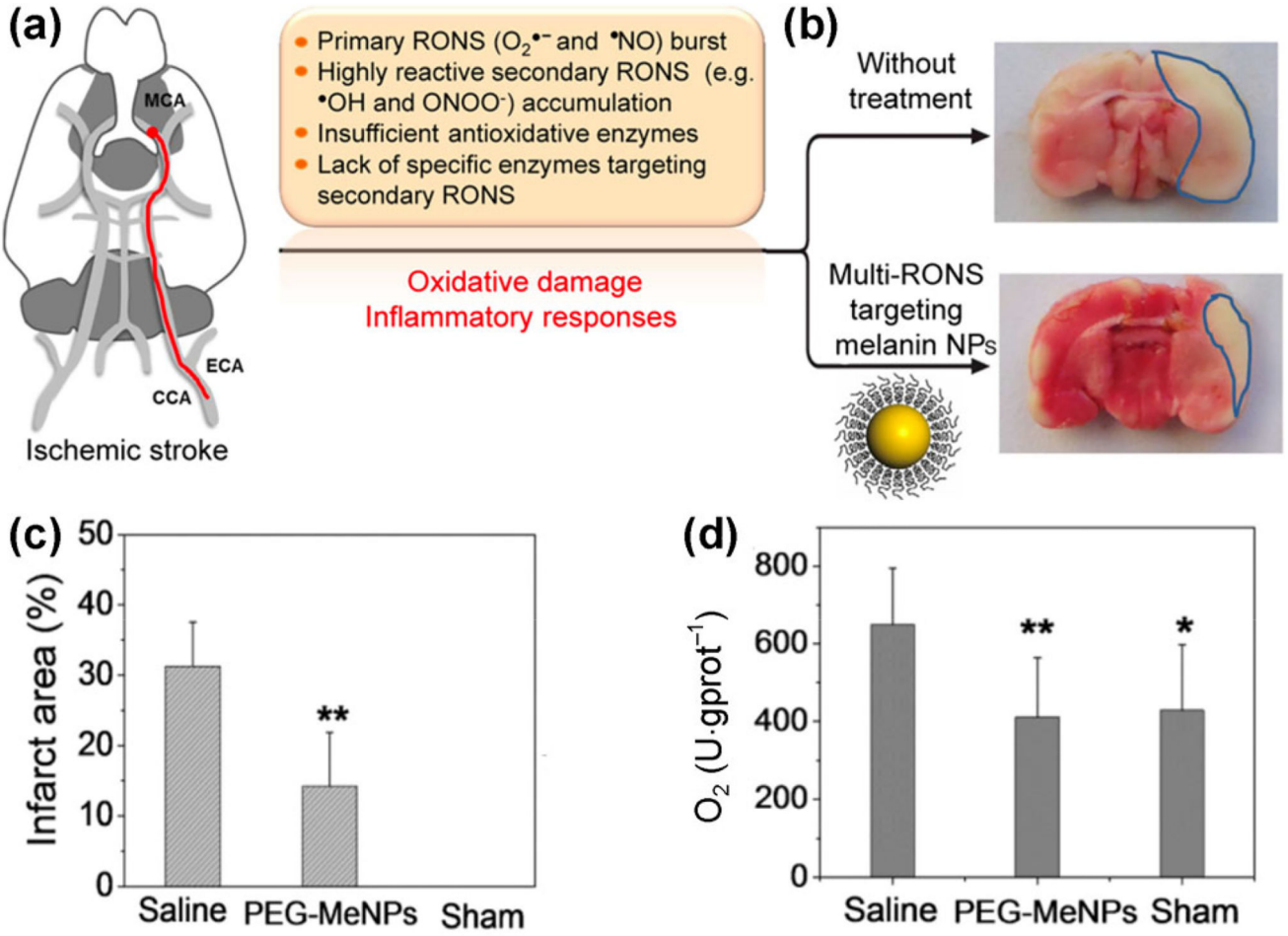

Figure 9.

(a) Schematic representation of the ischemic stroke model. (b) Representative images of TTC-stained brain slices from different groups. The corresponding (c) infarct areas and (d) $O_2^{\bullet-}$ levels in brain tissues of the three groups (*$p < 0.05$ and **$p < 0.01$ vs. saline control). Adapted with permission from Ref. [109], © American Chemical Society 2017.

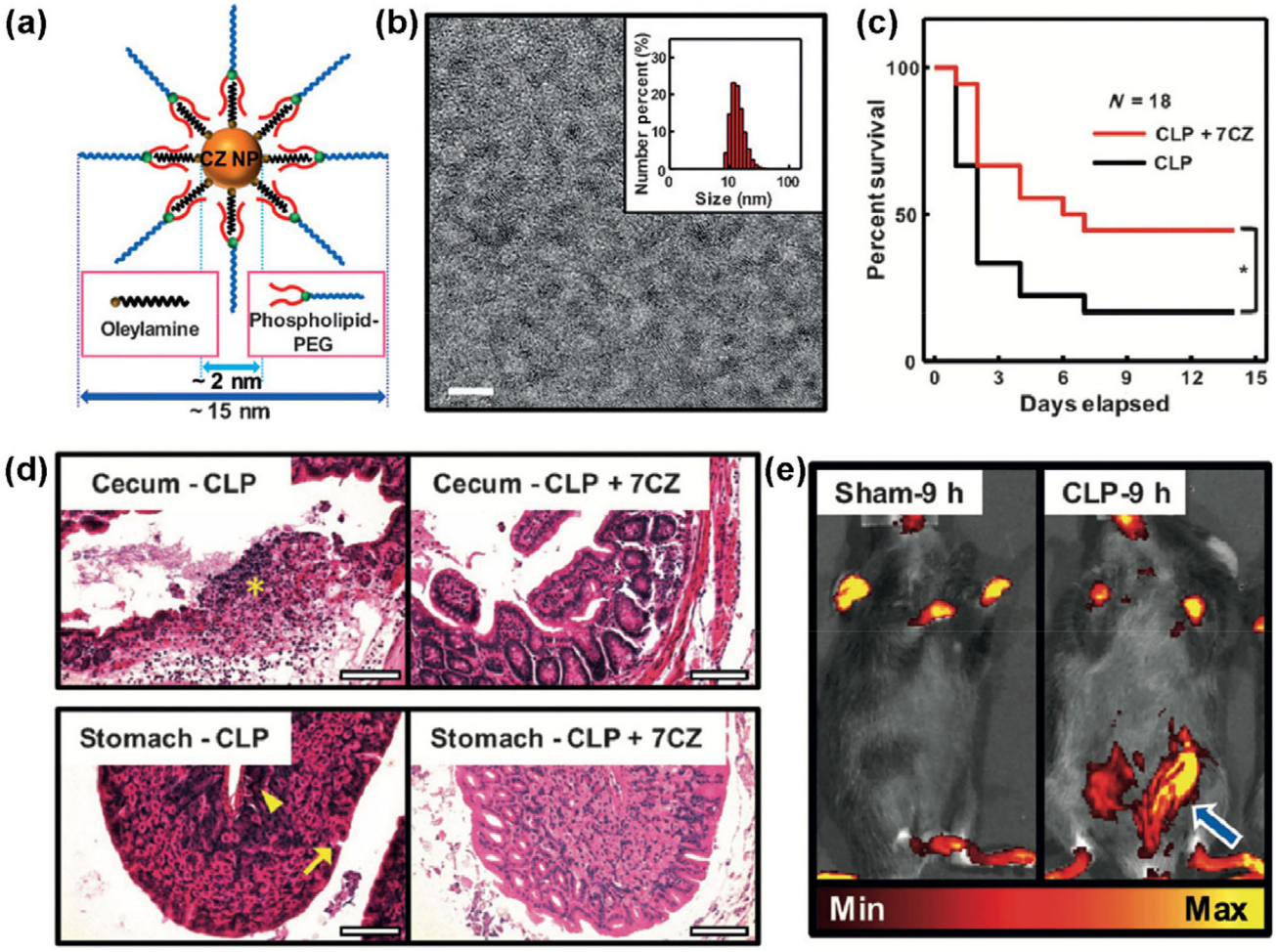

Figure 10.

(a) and (b) Illustration, characterization, and ROS-scavenging activities of ceria NPs and CZNPs. (a) Illustration of the structure of CZNPs. (b) TEM image of CZNPs; scale bar: 5 nm. (c) Mortality-reducing effects of CZNPs in the *in vivo* mouse model of CLP-induced bacteremia. After induction of CLP, PBS or CZNPs (2 $mg \cdot kg^{-1}$) were placed into the intraperitoneal space, and then the abdomen was sutured. Graph shows the survival curves in the CLP over 14 days; $n = 18$, $*p < 0.05$. (d) Representative histopathological images. Asterisk, ulcer detritus; arrow, mucosal disruption; arrowhead, mononuclear cell infiltration. Scale bars: 100 mm. (e) Representative *in vivo* near-infrared fluorescent optical images of the models 9 h after intravenous injection with Cy5.5-CZNPs. Colored signals denote Cy5.5 fluorescence (excitation = 620 nm, emission = 710 nm). Adapted with permission from Ref. [81], © John Wiley and Sons 2017.

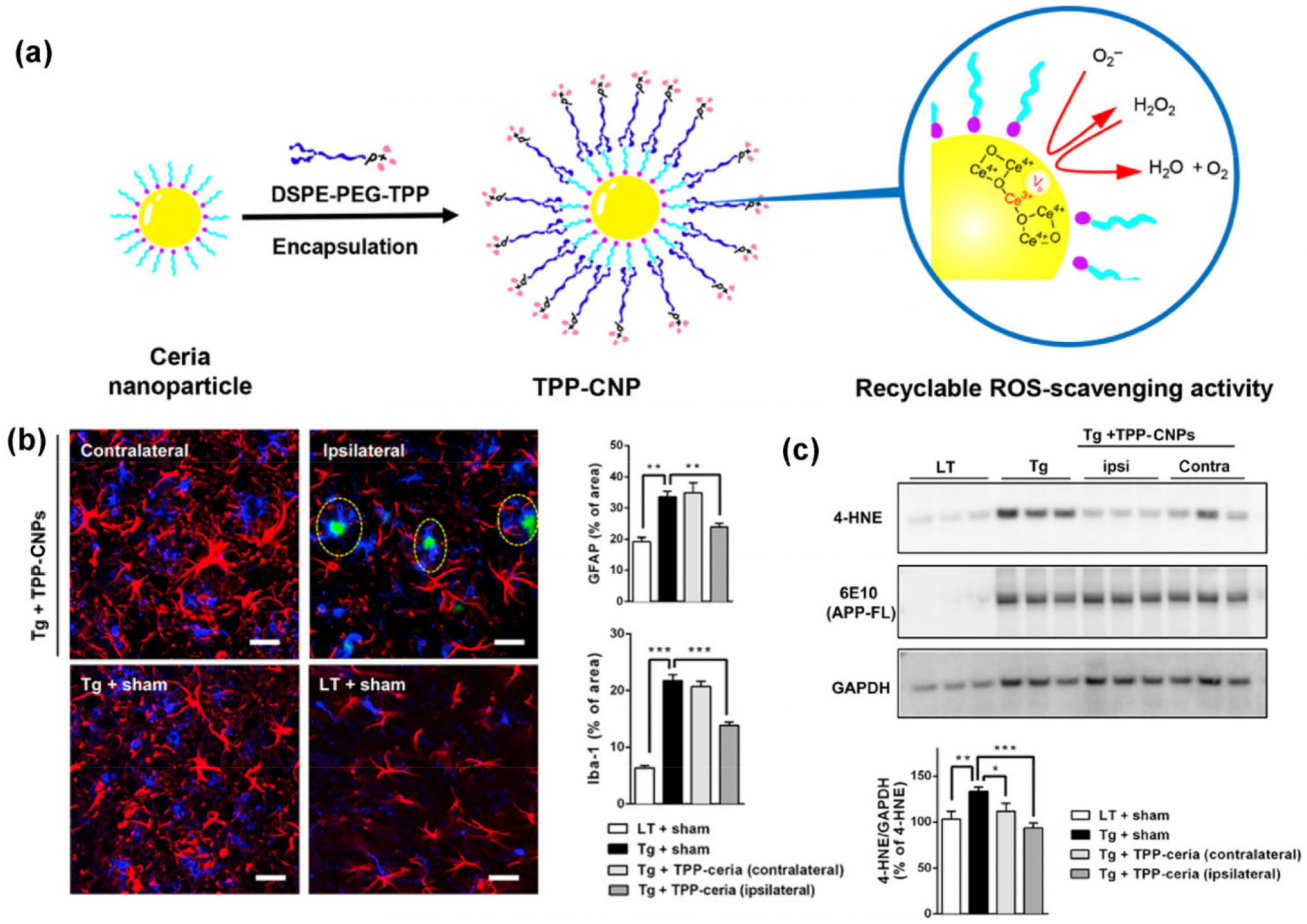

Figure 11.

(a) Design, synthesis, and characterization of TPP-CNPs as therapeutic mitochondrial antioxidants for the treatment of Alzheimer's disease. Scheme of DSPE-PEG-TPP-coated ceria nanoparticles exhibiting ROS recyclable scavenging activity. (b) TPP-CNPs reduce reactive glial activation. Confocal fluorescence images (left) of gliosis in tissue sections co-labeled with GFAP (red) and Iba-1 (blue). Quantified levels of GFAP and Iba-1 in the images ($n = 4$ per group). Statistical analysis was performed using ANOVA. Error bars represent 95% CIs. $^{**}p < 0.01$; $^{***}p < 0.001$; LT + sham: littermate mice; Tg + sham: 5XFAD mice. Scale bar = 30 μm. (c) Western blot analysis for oxidative stress markers in 5XFAD mice treated with TPP-CNPs ($n = 3$ per group). Data were normalized with respect to the signal of GAPDH. Statistical analysis was performed using ANOVA. Error bars represent 95% CIs. $^{*}p < 0.05$; $^{**}p < 0.01$; $^{***}p < 0.001$; LT + sham: littermate mice; Tg + sham: 5XFAD mice. Adapted with permission from Ref. [135], © American Chemical Society 2016.

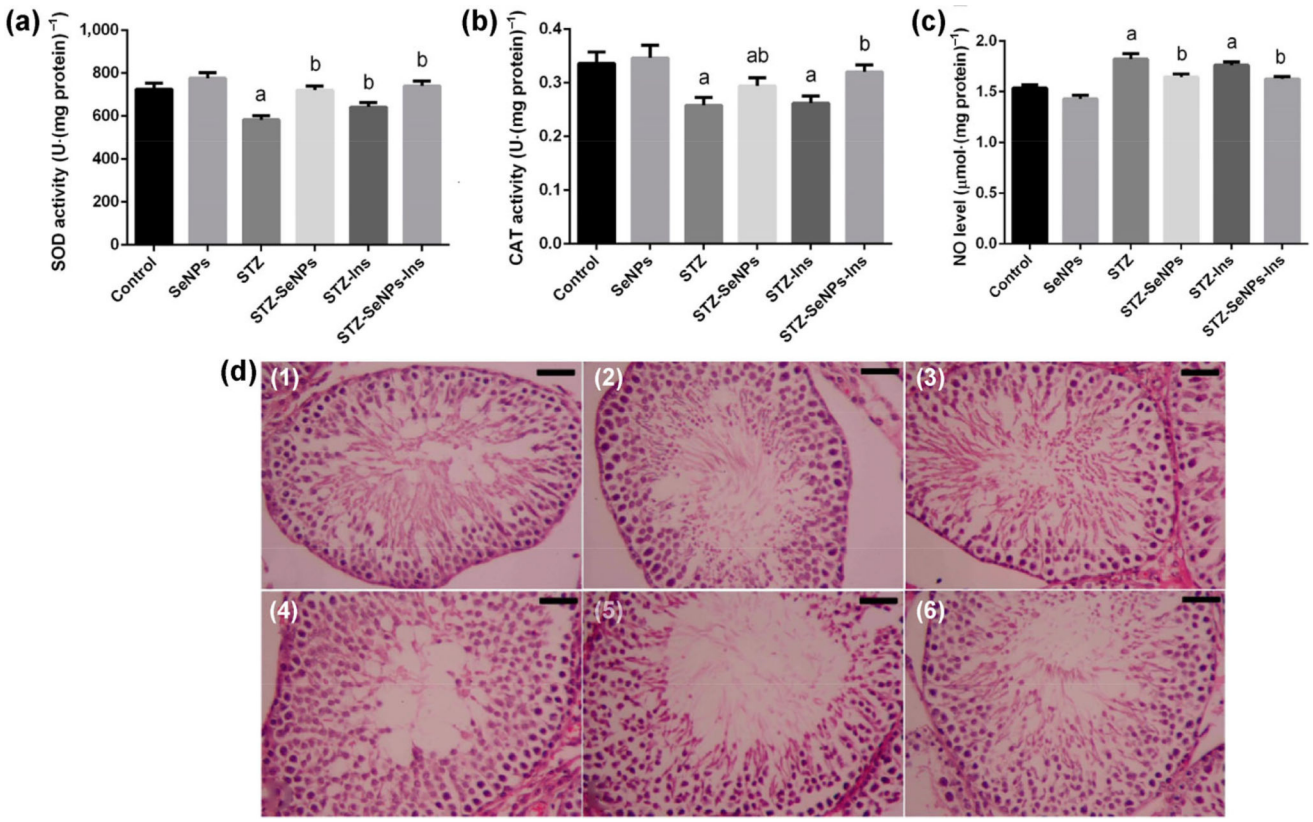

Figure 12.

(a)–(c) Effect of SeNPs and insulin on activities of the antioxidant enzymes ((a) superoxide dismutase: SOD and (b) catalase: CAT) in the testes of control and STZ-diabetic rats. (c) Impact of SeNPs and insulin on oxidative stress markers is shown by the levels of nitric oxide (NO) in the testes of control and STZ-diabetic rats. Values are mean ± SEM ($n = 7$). [a]$p < 0.05$, significant change with respect to Control group; [b]$p < 0.05$, significant change with respect to Diabetic group. (d) Impact of SeNPs and/or insulin on the morphology of the testes in diabetic rats. (1) control rats; showing typical testicular architecture; (2) SeNPs-treated rats; showing typical spermatogenic cells in the seminiferous tubules; (3) STZ-diabetic rats; showing severe testicular damage; (4) and (5) STZ-SeNPs-treated group, STZ-Ins-treated rats, and STZ-SeNPs-Ins-treated rats, respectively; SeNPs and/or insulin ameliorated the defects caused by diabetes in the spermatogenic cells of the seminiferous tubules. Tissues were stained with hematoxylin and eosin. Scale bar = 50 μm. Adapted with permission from Ref. [146] under the Creative Commons Attribution License, © Dkhil et al. 2016.

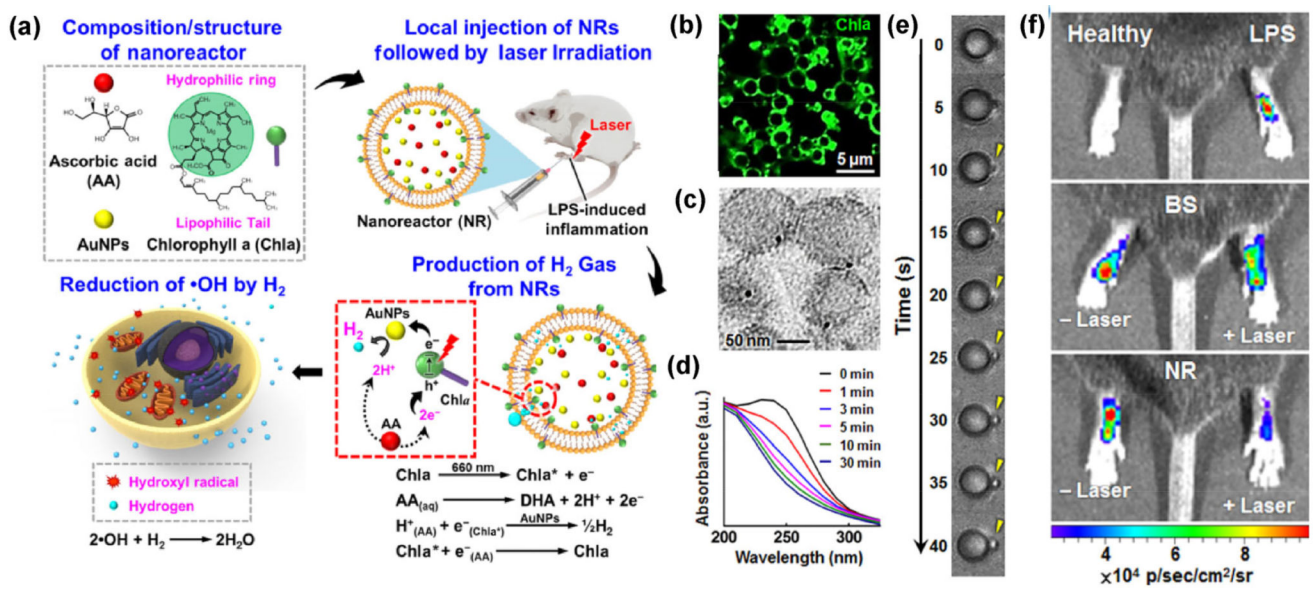

Figure 13.

(a) Composition/structure of a photodriven NR; mechanisms of using NR for photosynthesis of H_2 gas *in situ* to reduce oxidative stress in a mouse model of LPS-induced inflamed paw. (b) Fluorescence image of Chla embedded in Lip membrane of NR. (c) TEM image of AuNPs encapsulated in NR. (d) Spectral changes of AA encapsulated in NR after various periods of laser irradiation. (e) Bright-field images of H_2 bubbles generated in an NR following laser irradiation. (f) IVIS images of ROS in LPS-induced inflamed paws after treatment with BS and NR without/with laser irradiation. Adapted with permission from Ref. [153], © American Chemical Society 2017.

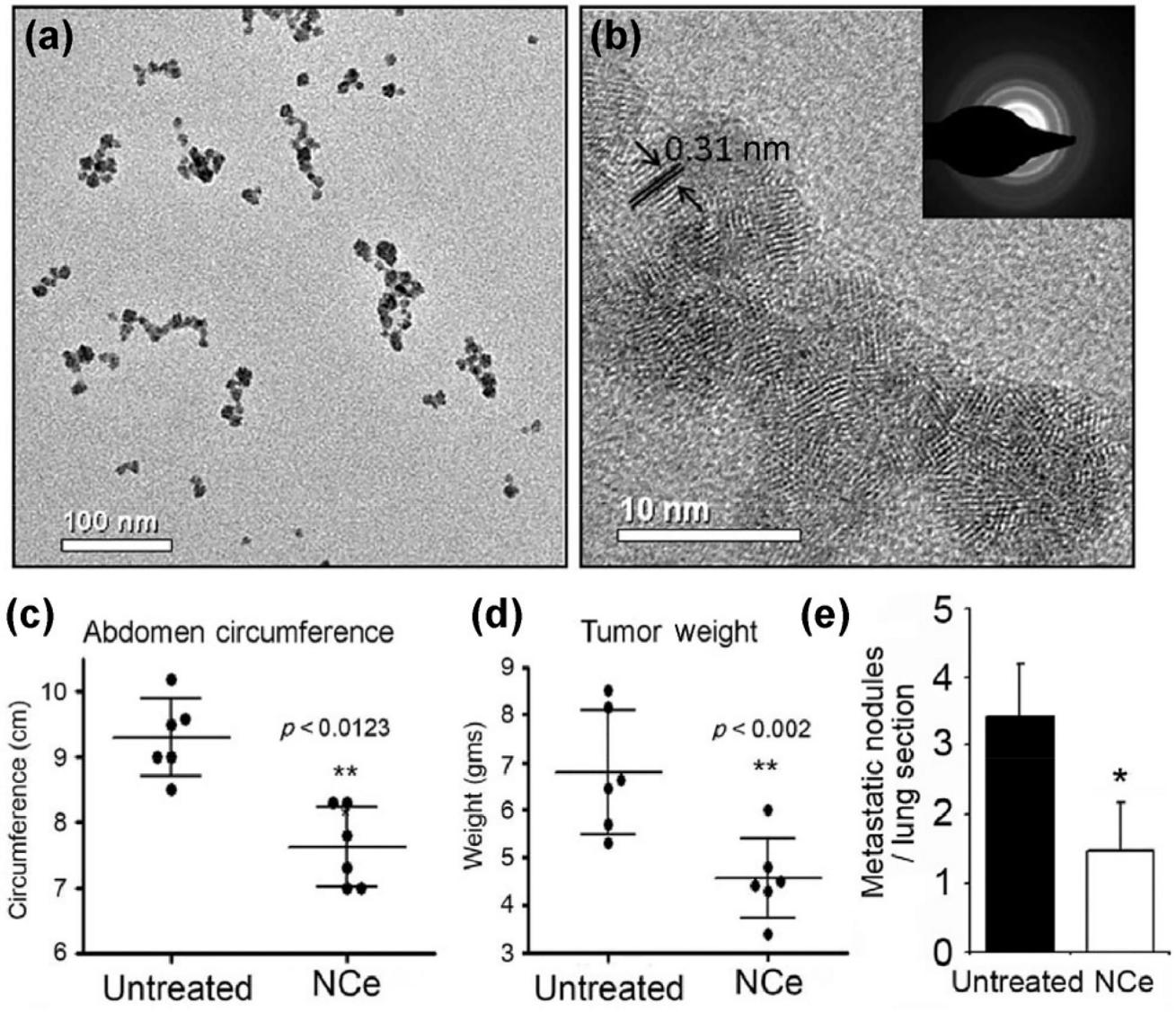

Figure 14.

High-resolution transmission electron micrographs show the presence of (a) loose agglomerates of 15–20 nm at low magnification and (b) individual 3–5 nm crystallites. The *d* spacing of 0.31 nm shows planes of ceria, while the selected area electron diffraction (SAED) pattern confirms the presence of fluorite lattice of cerium oxide. (c) Gross morphology of representative mouse with tumors at day 30 ($n = 6$). (d) Cumulative abdominal circumference measured at the end of the study. (e) Excised tumor weight from vehicle (PBS)-treated and NCe-treated mice (0.1 $mg \cdot kg^{-1}$ bd wt; every third day). Results are shown as mean ± S.D. of six individual animals. $^{**}p < 0.01$; NCe-treated groups were compared with untreated group using two-tailed Student's *t*-test (Prism). (f) Enumeration of metastatic nodules found per lung in untreated and NCe-treated mice. Total of five lung sections were observed to obtain the average count. $^{*}p < 0.005$; NCe-treated groups were compared with untreated group using two-tailed Student's *t*-test (Prism). Adapted with

permission from Ref. [164] under the terms of the Creative Commons Attribution License, © Giri et al. 2013.